

2nd

CR 114707
AVAILABLE TO THE PUBLIC

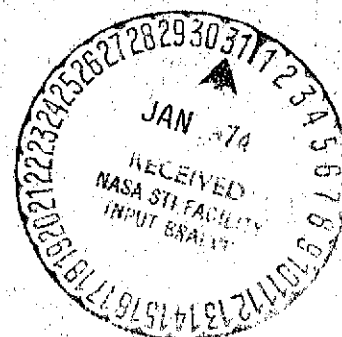
**Concepts for a Theoretical and Experimental
Study of Lifting Rotor Random Loads
and Vibrations**

Phase I Report under Contract NAS2-4151

**by Kurt H. Hohenemser
and Gopal H. Gaonkar**

**Department of Systems, Mechanical and
Aerospace Engineering**

**Washington University
School of Engineering and
Applied Sciences
St. Louis, Missouri**



September, 1967

(NASA-CR-114707) CONCEPTS FOR A
THEORETICAL AND EXPERIMENTAL STUDY OF
LIFTING ROTOR RANDOM LOADS AND
VIBRATIONS, PHASE I (Washington Univ.)
74 p HC \$5.75

N74-14755

CSC 01C

G3/02

Unclas
26987

Concepts for a Theoretical and Experimental
Study of Lifting Rotor Random Loads
and Vibrations

Phase I Report under Contract NAS2-4151 .

Prepared for the U. S. Army Aeronautical
Research Laboratory at Ames Research Center,
Moffet Field, California

by Kurt H. Hohenemser.
Kurt H. Hohenemser

and Gopal H. Gaonkar.
Gopal H. Gaonkar

Washington University
School of Engineering and
Applied Sciences
St. Louis, Missouri

September, 1967

Scope of Contract NAS2-4151

Work under Contract NAS2-4151 started on February 1, 1967 with the purpose "to define and study one or more probabilistic models for the computation of lifting rotor random dynamic loads and vibrations, which are suitable for the interpretation of wind tunnel and flight measurements of rotor loads and vibrations using power spectral density measuring techniques." This report summarizes the results obtained through August, 1967 when eight man-months of work had been expended. Work under subject contract, which extends through July, 1968 to a total of twenty-one man-months, is being continued.

Concepts for a Theoretical and Experimental
Study of Lifting Rotor Random Loads
and Vibrations

by Kurt H. Hohenemser
and Gopal H. Gaonkar

Washington University, St. Louis, Missouri

Abstract:

After briefly discussing a number of lifting rotor conditions with random inputs, the present state of random process theory, applicable to lifting rotor problems is sketched. Possible theories of random blade flapping and random blade flap-bending are outlined and their limitations discussed. A plan for preliminary experiments to study random flapping motions of a see-saw rotor is developed.

Concepts for a Theoretical and Experimental
Study of Lifting Rotor Random Loads
and Vibrations

Contents

	Page
Notation	
1. Introduction. The Significance of Lifting Rotor Random Loads	1
1.1 Lifting Rotor Response to Atmospheric Turbulence	
1.2 Stopping and Folding of Lifting Rotors in Flight	
1.3 Lifting Rotor Hovering Performance	
1.4 Unsteady Blade Aerodynamics	
1.5 Vertical Descent in the Vortex State	
1.6 Transition from Hovering to Forward Flight and Vice Versa	
2. Survey of Random Process Theory Related to Lifting Rotor Problems	6
2.1 General Remarks on Random Processes	
2.2 Response of a Constant Parameter Linear System to a Stationary Random Input	
2.3 Response of a Constant Parameter Linear System to a Non Stationary Random Input	
2.4 Response of a Time Variable Linear System to Random Inputs	
2.5 Response of Linear Systems to Multiple Random Inputs	

3.	Random Blade Flapping	17
3.1	Assumptions	
3.2	Small Advance Ratio	
3.3	Moderate Advance Ratio	
4.	Random Blade Flap-Bending	24
4.1	Derivation of Blade Stiffness Matrix	
4.2	Response Analysis with General Admittance Matrix	
4.3	Real Normal Mode Analysis	
4.4	Complex Normal Mode Analysis	
5.	Outline for Lifting Rotor Model Tests in Turbulent Flow	41
5.1	Model Tests with Both Load and Load Response Measurements	
5.2	Model Tests with Load Response Measurements Only	
6.	Conclusions	44
	References	
	Appendices	
<u>Appendix A</u>	Time Averaged Autocorrelation Function and Associated Power-Spectral Density of a Stationary Random Process Modulated by a Periodic Function	48
<u>Appendix B</u>	Computation of Power-Spectral Density for a Flapping Randomly Excited Blade	51
<u>Appendix C</u>	Discrete Element Algorithm for Complex Normal Mode Analysis of Multi Degree of Freedom Stable Systems Under Random Excitation . .	58

List of Figures:

Figure 1	Discrete element idealization for blade flap-bending . . .	26
Figures 2, a to d	Spectral density of flapping oscillations of rigid blades in forward helicopter flight, assuming the response to be a stationary random process modulated by periodic functions.	54

Notation for main report

$\mu_x = E[x]$	Expected value of sample x
$E[f(x)]$	Expected value of sample function $f(x)$
$x_1 = x_1(t_1), x_2 = x_2(t_2)$	Values of sample function $x(t)$ at times t_1 and t_2 respectively
$p(x_1), p(x_1, x_2)$	First and second order probability densities
t	Time
$\tau = t_2 - t_1$	Time difference
$t = \frac{t_1 + t_2}{2}$	Average time
$R_{xy}(t_1, t_2)$	Cross-correlation function between sample time functions $x(t_1)$ and $y(t_2)$
$f = \frac{\omega}{2\pi}$	Frequency
Δf	Frequency interval
$X(f)$	Fourier transform of sample function $x(t)$
$S_{xy}(f_1, f_2) = E[X^*(f_1)Y(f_2)]$	Cross-correlation function between sample frequency functions $X^*(f_1)$ and $Y(f_2)$, also called power spectral density
$\rho_{xy}(\tau) = \frac{R_{xy}(\tau)}{\sigma_x \sigma_y}$	Normalized cross-correlation function

$\sigma_x = \sqrt{E \left[(x - \mu_x)^2 \right]}$	Standard deviation of probability density $p(x)$
ν_a^+	Expected value of positive crossings per unit time of the level a
$h(\tau)$	Unit impulse response function
$H(f)$	Frequency response function
F	Modulating frequency
Ω	Rotor angular velocity
R	Rotor radius
μ	Advance ratio
β	Blade flapping angle, positive up
$\bar{\alpha}$	Mean blade angle of attack
α	Lift slope
c	Blade chord
γ	Blade inertia number
ρ	Air density
w	Vertical gust velocity
$S_{\bar{\alpha}}(f)$	Power spectral density of mean angle of attack
$\bar{S}_{\beta}(f)$	Average power spectral density of blade flapping angle

$$\left. \begin{array}{cc} a_1 & c_1 \\ a_2 & c_2 \\ a_3 & c_3 \end{array} \right\}$$

Constant coefficients in the blade flapping equation defined by eqn. 3.3.9

$B(f)$

Fourier transform of $\beta(t)$

$\bar{A}(f)$

Fourier transform of $\bar{\alpha}(t)$

EI

Blade bending stiffness

y

Vertical blade deflection, positive up

T

Blade axial tension force

m

Blade mass per unit length

r

Distance of blade station from rotor center

x_n

Distance from rotor center to midpoint of nth blade element

l_n

Length of nth blade element

m_n

Average mass of element n, concentrated at point x_n

y_n

Bending deflection at point x_n , positive up

c_n

Damping coefficient for blade element l_n , concentrated at point x_n

θ_n	Slope of blade element n
$(EI)_{n+1}$	Blade bending stiffness at point $x_n + \frac{l_n}{2}$
F_n	Average imposed force on blade element l_n , at point x_n
S_{n+1}	Shear force between blade elements n+1 and n, positive up on element n
T_{n+1}	Axial tension force between blade elements n+1 and n, positive in x direction on element n
M_{n+1}	Spring moment between blade element n+1 and n, positive, when counterclockwise on element n
K_{n+1}	Spring constant of spring between element n+1 and n
$[w]$	Influence coefficient matrix with element w_{jk}
$[k]$	Stiffness matrix with elements k_{jk}
$[I]$	Unit matrix
$[m]$	Mass matrix
$[c]$	Damping matrix
$\{f(t)\}$	Exciting force column with element f_k
λ	Complex natural frequency

$$[R^f(\tau)]$$

Force cross correlation matrix
with elements

$$R_{jk}^f(\tau) = E [f_j(t)f_k(t+\tau)]$$

$$[S^f(\omega)]$$

Force cross power spectral density
matrix with elements

$$S_{jk}^f(\omega) = E [F_j^*(\omega)F_k(\omega)]$$

$$\{F(\omega)\}$$

Fourier transforms of exciting
force column with element $F_k(\omega)$

$$[R^y(\tau)]$$

Deflection cross correlation matrix

$$[S^y(\omega)]$$

Deflection cross power spectral
density matrix

$$[A]$$

Modal matrix with elements $A_{j\nu}$,
where the latin subscript refers
to the station and the greek
subscript to the mode

$$[\omega^2]$$

Diagonal matrix of natural
frequency squares of system without
damping with elements ω_ν^2

$$[]^{-1}$$

Inverse of a matrix

$$[]^T$$

Transpose of a matrix

$$\{\}$$

Column vector

$$\{\}^T$$

Row vector

$[\mu]$	Diagonalized mass matrix with element μ_ν
$[x]$	Diagonalized stiffness matrix with element x_ν
$\{\eta\}$	Column of normal deflection coordinates with elements η_ν
$\{\varphi\}$	Column of normal force coordinates with elements φ_ν
$\{\zeta\}$	Column of normal damping over critical damping ratios with elements ζ_ν
$[M]$	Transformed mass matrix defined by eqn. 4.4.4
$[K]$	Transformed stiffness matrix defined by eqn. 4.4.5
$[S]$	Stress-deflection matrix
σ	Stress

Superscripts:

*	Conjugate complex
.	Time differentiation
-	Time average except in Section 4.4 where the bar denotes quantities in transformed equations for complex normal mode analysis

Notation in Appendices:

Appendix A:

$A(t)$	Periodic time function
$2\pi/\omega_0$	Period of periodic time function
c_k	Complex Fourier expansion coefficient

Appendix B:

$\theta_1, \theta_2, \theta_3$	Phase angles in generalized blade flapping equation defined by eqn. B-1
$\frac{\omega_0}{2\pi}$	Frequency interval
$n = \frac{\Omega}{\omega_0}$	A constant integer
$k = \frac{\omega}{\omega_0}$	Discrete variable
$S_k(\omega) = \bar{S}_\beta(k\omega_0)$	Average power spectral density of blade flapping angle at end of kth frequency interval

1. Introduction. The Significance of Lifting Rotor Random Loads

As of now the problem of lifting rotor dynamic loads and vibrations has been treated almost exclusively on the basis of deterministic modeling. In the most advanced treatment the flow field in the vicinity of the rotor is computed from the system of vortices generated by the blades, and the dynamic response of the blades is obtained by computing the interactions between the flow field and the blades. In comparing computed and measured dynamic loads and vibrations, it is necessary to assume stabilized flight conditions. Maneuver and gust dynamic loads and vibrations are treated as transients between stabilized conditions.

This deterministic model of the generation of dynamic lifting rotor loads and vibrations is in many respects unsatisfactory. Even under the steady flow conditions for lifting rotor models in wind tunnels the blades perform sizable random motions indicating the gross turbulent character of the rotor inflow. In flight this local turbulence of the inflow is superimposed to the atmospheric turbulence and to pilot control inputs which are both of a random nature. It would, therefore, seem appropriate to try to treat the problem of lifting rotor dynamic loads and vibrations with probabilistic modeling techniques. Such techniques have been successfully applied to the problem of airplane gust responses, see for example Ref. (1) and (2). Airplanes with known dynamic response characteristics are used to measure parts of the atmospheric turbulence spectra, and these spectra are then used to predict the gust responses of new prototype airplanes in the design stage. It is conceivable that an approach along these lines could be very useful for the prediction of lifting rotor dynamic loads and vibrations, though the problem is here much more involved than for airplanes, because of the numerous significant degrees of freedom and the complexity of the random phenomena associated with the rotary wing aircraft. It is rather surprising that apparently no previous efforts in this direction have been made although for some widely differing lifting rotor problems a description of

the underlying phenomena by random process is called for. The only indication that work in this area is planned was found in Ref. (3) which describes a test set-up suitable for measuring the response of a beam to lateral random loads.

The stochastic methods developed to analyze airplane responses to atmospheric turbulence or to define atmospheric turbulence by airplane response measurements are not applicable to lifting rotors for two reasons:

First, the coefficients of the equations of motion of lifting rotors are time variable rather than constant as for airplanes. Second, the widely made assumption that the vertical gust velocities over the wing span can be approximated by a single stationary random process is not valid for rotary wings. The rotor blade will have to be subdivided in a number of elements whereby the vertical velocity components at different elements will be represented by different non-stationary correlated random processes. The multiplicity and non-stationarity of the random processes associated with rotary wings invalidates the widely used relation according to which the ratio of output over input power spectral density equals the square of the system transfer function. Unlike airplanes, it will be necessary to consider variations of the turbulence spectrum along the span of the blade. The problem then would be to derive such a distribution of the turbulence spectrum over the blade span from the measured blade motions, or in a design situation, to derive the blade random vibrations from a given distribution of the turbulence spectrum over the blade span. For this reason neither the theoretical nor the experimental methods available for determining airplane responses to atmospheric turbulence can be adopted for lifting rotors, and new theoretical and experimental techniques must be developed.

Six types of lifting rotor problems where the application of random process concepts appears to be promising will be briefly discussed.

1.1 Lifting Rotor Response to Atmospheric Turbulence

In order to study the lifting rotor response to atmospheric turbulence one could think of testing a rotor model in a wind tunnel equipped with a gust generating system. Such a system has been installed in the NASA Langley Transonic Wind Tunnel and is described in Ref. (4). The system simulates a low amplitude continuous sinusoidal vertical gust. Under the usual assumption made for frozen wing aircraft - the vertical gust velocity can be represented by a single stationary random process - it is sufficient to measure the model response to sinusoidal vertical gusts over an adequate frequency range, since one needs only the system transfer function. For lifting rotors, however, for reasons explained before, the knowledge of the transfer function is not sufficient. The gust generator, in order to be applicable to lifting rotor models, must be capable of producing the entire gust spectrum with the proper amplitude ratios. No such device has apparently been designed or built anywhere as yet. Correspondingly, a theoretical computation of system transfer functions, as it is performed by the various sophisticated computer programs developed for lifting rotors, is also not adequate for the problem of lifting rotor response to atmospheric turbulence, and considerably more elaborate programs will have to be developed for this purpose.

1.2 Stopping and Folding of Lifting Rotors in Flight

The helicopter industry is vigorously working on problems of stopping and folding of lifting rotors in flight in an effort to develop air vehicles which combine the hovering efficiency of the helicopter with the cruising efficiency of high performance airplanes. Wind tunnel tests have been conducted to study the stopping and folding process of lifting rotor models in a steady flow. Because of the crucial effects of atmospheric turbulence these tests cannot be considered realistic. Even if the transfer functions were to be determined analytically or experimentally in a wind tunnel with low amplitude sinusoidal gust simulation, the results

could not be applied to the problem (except when the rotor is stopped) because of the frequency shifts produced by the time varying coefficients in the equations of motion. The solution of the problem requires new methods of analysis, and in an experimental approach the model must be subjected to often repeated stopping and starting conditions with a simulation of the full turbulence spectrum.

1.3 Lifting Rotor Hovering Performance

In spite of several decades of lifting rotor research and development, hovering performance prediction for new types of rotors is still quite poor. The widely accepted and continuously refined methods of performance prediction very often miss the mark by relatively large margins. A 10% overestimate of hovering performance is usually equivalent to 30 to 50% overestimate of payload and can have very serious consequences. It is also known that certain types of atmospheric turbulence can considerably degrade the helicopter OGE hovering performance.

Great progress has recently been made in the computation of the vortex wake system generated by a hovering lifting rotor. These computations, in agreement with test observations, have shown that the trailing vortices of one blade can get into the path of the subsequent blade whereby considerable drag increases and lift losses occur. The presence of atmospheric turbulence will amplify this tendency. A satisfactory definition and prediction of lifting rotor hovering performance should, therefore, include the effects of atmospheric turbulence and the associated random control inputs.

1.4 Unsteady Blade Aerodynamics

Another area of lifting rotor research where lately considerable progress has been made is that of unsteady blade aerodynamics, particularly in the region of partial blade stall. The unsteady stall phenomena are highly complex and very much dependent on the time history of blade angle of attack changes. Atmospheric turbulence will probably have a large effect on unsteady blade stall. Since the blade stall phenomena provide the forward speed limitation of most rotary wing

aircraft, theory and testing in this regime also seems to require the application of the concepts of random processes.

1.5 Vertical Descent in the Vortex State

Another flight condition where the lifting rotor loads are basically of a random nature, is the descent in the vortex state. Both rigid and flapping rotors show large thrust variations beginning at quite small vertical descent rates and becoming maximum at the fully developed vortex state inflow pattern. Such thrust variations have been described for example in Ref. (5). A theory using random process concepts would appear to be suitable for this flight condition.

1.6 Transition from Hovering to Forward Flight and Vice Versa

It is well known that most helicopters have a slow speed range corresponding to advance ratios between .05 and .10 where dynamic blade loads and vibrations are much higher than in cruising flight. Take-off and landing maneuvers fall into this slow speed range and contribute to the high level of dynamic loads and vibrations. Flow through the rotor disk is strongly non uniform and wake recirculation takes place. No adequate deterministic theory of this complex flow state has been established as yet. The transition phenomenon also appears to be a promising candidate for the application of random process theory.

The preceding six cases where lifting rotor responses to random inputs are of importance are by no means exhaustive. It is also not at all obvious how to approach these problems. Their listing here has merely the purpose to provide some motivation to the search for suitable methods of treating lifting rotor random loads and vibrations.

2. Survey of Random Process Theory Related to Lifting Rotor Problems

Random process theory so far has been predominantly applied in communication and automatic control engineering. Its application to mechanical systems and structures is still quite limited. A number of good textbooks on random process theory and measurements have recently been published, for example Ref. (6) and (7), and some modern textbooks on mechanical vibrations contain a chapter on the response of structures to random inputs, see for example Ref. (8). Most of the literature deals with constant parameter linear systems subjected to a stationary random input. Very little work exists on non stationary random inputs as they occur in lifting rotors, and no previous work was found on the computation of responses of time varying linear systems to random inputs which is required in the random flapping and flap-bending analysis of lifting rotor blades. The response of complex structures with many degrees of freedom subjected to multiple correlated random inputs has only very recently been treated in a few papers, see for example Ref. (9) and (10), and the best approach to this problem which must be solved for the lifting rotor, is by no means obvious. This section gives a brief survey of random process theory as related to lifting rotor problems.

2.1 General Remarks on Random Processes

A random process is defined as an ensemble of random sample functions $x(t)$ which can be described by a variety of probabilistic measures. The first order probability $p(x_1)$ gives the distribution of $x_1 = x(t_1)$ over the ensemble at the time t_1 . For the sake of simplicity we will assume here that the expectation or mean value of $x(t)$ is always zero:

$$\mu_x = E[x(t)] = \int_{-\infty}^{\infty} xp(x)dx = 0 \quad 2.1.1$$

The second order probability $p(x_1, x_2)$ gives the joint distribution of $x_1 = x(t_1)$ and $x_2 = x(t_2)$ at the times t_1 and t_2 . The expectation of the product $x_1 x_2$ is called the autocorrelation function $R_x(t_1, t_2)$

$$R_x(t_1, t_2) = E[x_1 x_2] = \iint_{-\infty}^{\infty} x_1 x_2 p(x_1, x_2) dx_1 dx_2 \quad 2.1.2$$

and is in general a function of both t_1 and t_2 .

Higher order probabilities $p(x_1, x_2, x_3, \dots)$ and higher moments $E[x_1 x_2 x_3 \dots]$ can be defined and are necessary for a complete description of a random process. Usually one limits the description to the first and second order probabilities. For the special case of a normal or Gaussian process, such a description is complete.

In the case of two correlated random processes with sample functions $x(t)$ and $y(t)$ there exists a second order joint probability $p(x_1, y_2)$, where $x_1 = x(t_1)$; $y_2 = y(t_2)$. The expectation of the product $x_1 y_2$ is called the cross-correlation function $R_{xy}(t_1, t_2)$

$$R_{xy}(t_1, t_2) = E[x_1 y_2] = \iint_{-\infty}^{\infty} x_1 y_2 p(x_1, y_2) dx_1 dy_2 \quad 2.1.3$$

We now introduce the complex sample Fourier transforms of the sample functions $x(t), y(t)$

$$\begin{aligned} X(f) &= \int_{-\infty}^{\infty} x(t) e^{-i2\pi f t} dt \\ Y(f) &= \int_{-\infty}^{\infty} y(t) e^{-i2\pi f t} dt \end{aligned} \quad 2.1.4$$

with their inverse

$$\begin{aligned} x(t) &= \int_{-\infty}^{\infty} X(f) e^{i2\pi f t} df \\ y(t) &= \int_{-\infty}^{\infty} Y(f) e^{i2\pi f t} df \end{aligned} \quad 2.1.5$$

The probabilistic measure in the frequency domain which is equivalent to $R_{xy}(t_1, t_2)$ in the time domain is the expectation of the product of complex sample Fourier transforms $E[X^*(f_1)Y(f_2)]$ which is called the double frequency cross-spectral density. It can be shown that it is related to the cross-correlation function by

$$S_{xy}(f_1, f_2) = E[X^*(f_1)Y(f_2)] = \iint_{-\infty}^{\infty} R_{xy}(t_1, t_2) e^{i2\pi(f_1 t_1 - f_2 t_2)} dt_1 dt_2 \quad 2.1.6$$

The inverse relation between cross-correlation function and double frequency cross-spectral density is given by

$$R_{xy}(t_1, t_2) = \iint_{-\infty}^{\infty} S_{xy}(f_1, f_2) e^{-i2\pi(f_1 t_1 - f_2 t_2)} df_1 df_2 \quad 2.1.7$$

The corresponding relations between auto-correlation function and power spectral density are obtained by replacing R_{xy} by R_x , S_{xy} by S_x and $Y(f_2)$ by $X(f_2)$.

Random processes are called weakly stationary if the first order probabilities are independent of time and if auto-correlation and cross-correlation functions depend only on the time difference $\tau = t_2 - t_1$ and not on $t_1 + t_2$. In this case one can prove the inequality

$$|R_{xy}(\tau)|^2 \leq R_x(0)R_y(0) \quad 2.1.8$$

which allows to define the normalized cross-correlation function

$$\rho_{xy}(\tau) = \frac{R_{xy}(\tau)}{\sqrt{R_x(0)R_y(0)}} = \frac{R_{xy}(\tau)}{\sigma_x \sigma_y} \quad 2.1.9$$

where σ_x and σ_y are the standard deviations of the time independent probability distributions $p(x)$ and $p(y)$. For $x = y$ one obtains

$$|R_x(\tau)| \leq |R_x(0)| = \sigma_x^2 \quad 2.1.10$$

If in the time domain $R_{xy}(t_1, t_2)$ depends only on $\tau = t_2 - t_1$ and not on $t_1 + t_2$, it can be shown that in the frequency domain $S_{xy}(f_1, f_2)$ also reduces to a function of a single frequency given by

$$S_{xy}(f) = E [X^*(f)Y(f)] = \int_{-\infty}^{\infty} R_{xy}(\tau) e^{-i2\pi f\tau} d\tau \quad 2.1.11$$

For $x = y$ this reduces to

$$S_x(f) = E [X^*(f)X(f)] \quad 2.1.12$$

In words: The power spectral density of a stationary random process is the expectation of the product of a sample Fourier transform with its conjugate complex value.

If the expected values taken over the ensemble of random functions are equal to the corresponding time averages taken over a sample function, the stationary process is called ergodic. In this case

$$R_{xy}(\tau) = E [x_1 y_2] = \lim_{T \rightarrow \infty} \frac{1}{2T} \int_{-T}^T x(t) y(t+\tau) dt \quad 2.1.13$$

While the double frequency power spectral densities of non-stationary random processes cannot be measured unless an entire ensemble of random functions is available, $S_{xy}(f)$ and $S_x(f)$ for stationary ergodic processes are measurable, if only a

single sample function is given. In order to obtain $S_x(f)$ one merely has to send the signal from a random sample function through a narrow band pass filter with the center frequency f and band width Δf and square and average it over an adequately long time period and divide the result by Δf .

For a ergodic process - again assuming zero mean value of the random function - the standard deviation σ_x of the probability distribution can be expressed either by the value of the autocorrelation function for $\tau = 0$ or by the integral over the power spectral density:

$$\sigma_x^2 = \int_{-\infty}^{\infty} x^2 p(x) dx = \lim_{T \rightarrow \infty} \frac{1}{2T} \int_{-T}^T x^2(t) dt = R_x(0) = \int_{-\infty}^{\infty} S_x(f) df \quad 2.1.14$$

Thus, for an ergodic process, the standard deviation of the probability distribution over the ensemble of random functions at any given time t equals the root mean square value taken over any sample function and can be obtained also by integrating over the power spectral density distribution. For an ergodic random process the time rate of the random function is uncorrelated to the function value at the same time. The standard deviation of the time rate is given by either one of the 4 expressions:

$$\sigma_{\dot{x}}^2 = \int_{-\infty}^{\infty} \dot{x}^2 p(\dot{x}) d\dot{x} = \lim_{T \rightarrow \infty} \frac{1}{2T} \int_{-T}^T \dot{x}^2(t) dt = -\ddot{R}_x(0) = \int_{-\infty}^{\infty} (2\pi f)^2 S_x(f) df \quad 2.1.15$$

An important concept applicable to the fatigue of structures under random loads is the expected number of crossings of a certain level per unit time. For a normal random process one can show that the expected value of positive crossings per unit time of the level a is given by

$$\nu_a^+ = \frac{1}{2\pi} \frac{\sigma_{\dot{x}}}{\sigma_x} e^{-\frac{a^2}{2\sigma_x^2}} \quad 2.1.16$$

Making use of the two preceding equations the expected value of positive zero crossings ($a = 0$) per unit time is

$$\nu_0^+ = \frac{1}{2\pi} \frac{\int_{-\infty}^{\infty} (2\pi f)^2 S_x(f) df}{\int_{-\infty}^{\infty} S_x(f) df} \quad 2.1.17$$

For a narrow band process almost every positive zero crossing leads to a full cycle, so that this equation, when applied to narrow band processes, also gives the expected value of cycles per unit time which is important in fatigue considerations.

2.2 Response of a Constant Parameter Linear System to a Stationary Random Input

A linear dynamic system with constant parameters can be described by the unit impulse response function $h(\tau)$. For a general input $x(t)$ the system response is then given by the convolution integral

$$y(t) = \int_0^{\infty} h(\tau) x(t-\tau) d\tau \quad 2.2.1$$

Taking the Fourier transform on both sides of this equation results in the relation

$$Y(f) = H(f)X(f) \quad 2.2.2$$

where

$$H(f) = \int_{-\infty}^{\infty} h(\tau) e^{-i2\pi f\tau} d\tau \quad 2.2.3$$

is the complex frequency response function of the system.

For stationary ergodic random inputs one determines the response auto-correlation function by taking the expected value of the product $y(t)y(t+\tau)$. With the help of the convolution integral this results in the following relation between input and response auto-correlation function:

$$R_y(\tau) = \iint_0^\infty h(\xi)h(\eta)R_x(\tau+\xi-\eta)d\xi d\eta \quad 2.2.4$$

The corresponding relation in the frequency domain is

$$S_y(f) = |H(f)|^2 S_x(f) \quad 2.2.5$$

All terms in this simple equation are real. The response standard deviation is given by

$$\sigma_y^2 = \int_{-\infty}^{\infty} |H(f)|^2 S_x(f) df \quad 2.2.6$$

and σ_y is again equal to the root mean square value taken over a sufficiently long time period of a sample response function.

The relation according to which the response power spectral density is equal to the input power spectral density multiplied by the square of the complex frequency response function is very widely used in many applications of random process theory. However, its validity is strictly limited to the case of a constant parameter linear system with a single stationary ergodic random input.

2.3 Response of a Constant Parameter Linear System to a Non Stationary Random Input

A general solution of this problem has been developed by Caughey in Ref. (11) in form of complex double and triple integrals. The practical problem is that, except in special cases, the complex double frequency power spectra associated with non stationary random processes, cannot be measured with a single sample function, since it takes the entire ensemble of functions to define the variation of its probabilistic measures with time. There are, however, two special cases where the power spectral densities associated with non stationary random processes can be defined and measured when only a single sample function is available. In both cases the non stationarity is due to a deterministic time trend. Such phenomena have been treated in Ref. (12).

In the first case the time trend is slow as compared to the random instantaneous fluctuations, so that the probabilistic measures can be determined with a single sample function by selecting an averaging time which is sufficiently long to obtain statistically meaningful values for the autocorrelation function or power spectral density but which is sufficiently short to exclude substantial effects of the slow time trend. Random processes which allow such measuring procedures are called locally stationary.

In the second case the deterministic time trends are periodic so that time averages of autocorrelation function and power spectral density can be defined. Since this case is important in lifting rotor theory it will be discussed here in more detail. We assume that $x(t)$ is a sample function of a stationary ergodic random process and we would like to know the average autocorrelation function and the power spectral density of the modulated random sample function $y(t)$ defined by

$$y(t) = x(t)\cos 2\pi Ft \quad 2.3.1$$

The autocorrelation function is:

$$\begin{aligned} R_y(t_1, t_2) &= E[x(t_1)x(t_2)] \cos 2\pi Ft_1 \cos 2\pi Ft_2 \\ &= (1/2)R_x(\tau)(\cos 2\pi F\tau + \cos 2\pi F(t_1+t_2)) \end{aligned} \quad 2.3.2$$

where $\tau = t_2 - t_1$.

Averaging over a sufficiently long time period, the last term will disappear and one obtains for the time averaged autocorrelation function

$$\bar{R}_y(\tau) = (1/2)R_x(\tau)\cos 2\pi F\tau \quad 2.3.3$$

The average autocorrelation function of the modulated stationary random function $x(t)$ is obtained by multiplying $R_x(\tau)$ with $(1/2)\cos 2\pi F \tau$.

The corresponding power spectral density can be either obtained by using the relation

$$\bar{S}_y(f) = \int_{-\infty}^{\infty} \bar{R}_x(\tau) e^{-i2\pi f\tau} d\tau \quad 2.3.4$$

or by taking the Fourier transform $Y(f)$ of $y(t)$ and inserting it in the definition

$$\bar{S}_y(f) = E [Y^*(f)Y(f)] \quad 2.3.5$$

The result is in either case

$$\bar{S}_y(f) = (1/4) [S_x(f-F) + S_x(f+F)] \quad 2.3.6$$

This power spectral density would be measured if a sample function $y(t)$ were analyzed in the usual way by sending the signal through a band pass filter with a band width Δf which is small as compared to F and by squaring and time averaging over a time which is large as compared to $1/F$. If the response power spectral density of the constant parameter linear system with the forcing function $y(t)$ were determined in the same way, it would be given by $|H(f)|^2 \bar{S}_y(f)$, where $H(f)$ is again the complex frequency response function of the system.

2.4 Response of Time Variable Linear Systems to Random Inputs

A linear system with time varying parameters - like a lifting rotor flapping blade - can be described by the unit impulse response function, which now is not only dependent on the time τ elapsed since applying the unit impulse, but also on the time t at which the impulse had been applied: $h(\tau, t)$.

In general the computation of $h(\tau, t)$ is not possible in closed form and numerical methods are required to find approximate solutions. For a general input $x(t)$ the system response is again given by the convolution integral

$$y(t) = \int_0^{\infty} h(\tau, t)x(t-\tau)d\tau \quad 2.4.1$$

The frequency response function is also time variable and determined by

$$H(f, t) = \int_{-\infty}^{\infty} h(\tau, t)e^{-i2\pi f\tau} d\tau \quad 2.4.2$$

Taking the expected value of the product $y(t_1)y(t_2)$ one obtains with the help of the convolution integral the following relation between input and response autocorrelation function:

$$R_y(t_1, t_2) = \iint_{-\infty}^{\infty} h(\xi, t_1)h(\eta, t_2)R_x(t_1-\xi, t_2-\eta)d\xi d\eta \quad 2.4.3$$

The corresponding relation in the frequency domain is

$$S_y(f_1, f_2) = \iint_{-\infty}^{\infty} S_x(\xi, \eta)J^*(\xi, \xi-f_1)J(\eta, \eta-f_2)d\xi d\eta \quad 2.4.4$$

where

$$J(\xi, f) = \int_{-\infty}^{\infty} H(\xi, t)e^{i2\pi ft}dt \quad 2.4.5$$

Apparently no attempt has been made as yet to solve these equations for an actual problem. A solution would be extremely difficult, since already the unit impulse response $h(\tau, t)$ is not given analytically but must be approximated by numerical

methods. The solution then requires triple infinite integrals over non analytical complex functions. Furthermore, as mentioned before, the input and output double frequency power spectra cannot be measured with a single sample function. However, if the variable parameter system is electronically simulated the input-output relation for power spectral densities can be experimentally observed under certain conditions.

2.5 Response of Linear Systems to Multiple Random Inputs

The application of random process theory to complex structures with multiple random inputs - even assuming stationarity - has not as yet progressed to a point where a good understanding of the various possible and necessary approximations has been achieved. The problem of random blade flap bending is therefore presented in Section 4 in considerable detail. A substantial simplification is possible if, as usually assumed, the damping of the structure is small so that normal mode cross damping terms can be neglected. Unfortunately, lifting rotor blades have large aerodynamic damping at least in the low frequency modes and not all cross damping terms are negligible. In this case, it may be simpler to transform the second order differential equations of the structure into an equivalent system of first order equations with respect to time. The normal modes are then complex and more difficult to handle, but the frequency response function is much simpler than for a second order system. Section 4 includes the general solutions both for a second order representation with real normal modes and for a first order representation with complex normal modes.

3. Random Blade Flapping

For sufficiently slow excitation the lifting rotor blade will respond mainly in its fundamental mode, that is in the blade flapping mode. For blades attached to the hub with flapping hinges, this is a rigid blade mode. For blades without flapping hinges the mode involves flap bending, however, in first approximation one can substitute rigid flapping about an off-set hinge. In the following a very simple analytical blade model is assumed which is adequate to discuss the basic problems of a random loads and vibration analysis.

3.1 Assumptions

It is assumed that the atmospheric turbulence affecting lifting rotor blade flapping consists of vertical velocity fluctuations which are uniform over the rotor span and which have a wave length which is large as compared to the effective rotor diameter. This type is called one-dimensional isotropic turbulence and is frequently used for airplane turbulence response calculations, see for example p. 21 of Ref. (1).

In a first order blade flapping theory valid for small flapping angles β , zero flapping hinge off-set and for moderate advance ratios μ , one obtains the following equation of motion (see for example Ref. (13), eqn. (15))

$$\ddot{\beta} + \frac{\gamma}{8} \left(1 + \frac{4}{3} \mu \sin t\right) \dot{\beta} + \left(1 + \frac{\gamma \mu}{6} \cos t\right) \beta = \frac{\gamma \bar{\alpha}}{8} \left(1 + \frac{8}{3} \mu \sin t\right) \quad 3.1.1$$

The equation has been linearized both with respect to the flapping angle β and with respect to the rotor advance ratio μ . The time unit has been selected so that the rotor angular velocity Ω is one. The only blade parameter in the equation is the non-dimensional blade inertia number γ which for practical rotors has values between 2 and 10. Actually, the blade angle of attack α should vary both with radius and with azimuth angle. However, in this simple mathematical model an average

value $\bar{\alpha}$ has been assumed which is independent of radius and blade azimuth angle and which is directly proportional to the vertical gust velocity. Using $.7R$ as effective rotor radius, the relation between vertical gust velocity w and $\bar{\alpha}$ is:

$$\bar{\alpha} = \frac{w}{.7 \Omega R} \quad 3.1.2$$

Thus, the average angle of attack $\bar{\alpha}$ directly reflects the atmospheric turbulence and is under the usual assumptions a stationary random function.

The stationary random process $\bar{\alpha}$, according to the blade flapping differential equation, is modulated by the deterministic time function $(1 + \frac{8}{3} \mu \sin t)$ and this non-stationary random input acts on a linear system with periodically varying parameters. In a more refined analysis considering the variability of the angle of attack with radius and with blade azimuth, $\bar{\alpha}$ would be replaced by the product of w with a deterministic time function.

From the physical aspects of the problem it is clear, that the assumption of a locally stationary process, discussed in Section 2.3 is not satisfied for β or $\bar{\alpha} \sin t$. The time trends from $\sin t$ and $\cos t$ are not slow as compared to the gust velocity fluctuations.

3.2 Small Advance Ratio

For small advance ratio μ the periodicity of the parameters in the blade flapping equation can be neglected. In this case the average power spectral density of the random input can be easily computed, since the modulated angle of attack $\bar{\alpha} \sin t$ has the average power spectral density

$$1/4 \left[S_{\bar{\alpha}} \left(f - \frac{1}{2\pi} \right) + S_{\bar{\alpha}} \left(f + \frac{1}{2\pi} \right) \right] \quad 3.2.1$$

see Section 2.3 (the relation given in Section 2.3 for the modulating function $\cos 2\pi F t$ is also valid for $\sin 2\pi F t$).

If $H(f)$ is the complex frequency response function for the blade, which, for constant parameters, has the value

$$H(f) = \frac{1}{-(2\pi f)^2 + 12\pi f \frac{\gamma}{8} + 1} \quad 3.2.2$$

one obtains for the average power spectral density of the flapping angle β the value:

$$\bar{S}_\beta(f) = |H(f)|^2 \left[\left(\frac{\gamma}{8}\right)^2 S_{\bar{\alpha}}(f) + \frac{1}{4} \left(\frac{\gamma\mu}{3}\right)^2 \left\{ S_{\bar{\alpha}}\left(f - \frac{1}{2\pi}\right) + S_{\bar{\alpha}}\left(f + \frac{1}{2\pi}\right) \right\} \right] \quad 3.2.3$$

In the absence of a solution for periodically varying parameters it is not possible to quantitatively establish the advance ratio range μ for which the above solution is a good approximation. It would appear, however, that an advance ratio of $\mu = .1$ should show a negligible effect of the μ -terms in the factors of β and $\dot{\beta}$. It is noteworthy that this advance ratio range includes the region of transition from hovering to forward flight and vice versa, during which considerable random loads and vibrations are encountered.

3.3 Moderate Advance Ratio

Inasmuch as up to now the only non stationary random processes which are analytically manageable are stationary processes which are modulated by a time function (such processes are treated in Ref. (12)), one might try to find a solution to the blade flapping equation 3.1.1 by assuming that the flapping angle β represents a stationary random process multiplied by a periodic time function. Since the input random process is of this type it may not be unreasonable to expect that at least to a certain approximation the response random process is of the same type. When time averaging the autocorrelation function of such a process one finds that the result depends only on $\tau = t_2 - t_1$, not on t_1 or t_2 , same as for

stationary random processes. In the frequency domain, time averaging amounts to multiplying the double frequency power spectral density with the delta function $\delta(f_2-f_1)$, thus reducing it to a single frequency power spectral density. This is shown for the general case of a periodic modulating function in Appendix A. Here we will consider the special case

$$y(t) = x(t)\cos 2\pi Ft \quad 3.3.1$$

treated in Section 2.3. $x(t)$ is again a sample function of a stationary random process. According to eqn. 2.1.6 the power spectral density for $y(t)$ is:

$$S_y(f_1, f_2) = E \left[Y^*(f_1) Y(f_2) \right] \quad 3.3.2$$

Applying the postulated rule, that time averaging corresponds in the frequency domain to multiplication of the double frequency power spectral density with $\delta(f_2-f_1)$, one obtains for the power spectral density of the random process with time averaged autocorrelation function

$$\bar{S}_y(f_1) = S_y(f_1, f_2) \delta(f_2-f_1) \quad 3.3.3$$

$$\text{or} \quad \bar{S}_y(f) = E \left[Y^*(f) Y(f) \right] \quad 3.3.4$$

$$\text{Since} \quad Y(f) = 1/2(X(f+F)+X(f-F)) \quad \text{and} \quad 3.3.5$$

$$\text{since} \quad E \left[X^*(f+F) X(f-F) \right] = 0 \quad 3.3.6$$

one obtains

$$\bar{S}_y(f) = 1/4 \left[S_x(f+F) + S_x(f-F) \right] \quad 3.3.7$$

in agreement with eqn. 2.3.6. In particular, we have for the power spectral density of the time averaged random process the rule, that the sample Fourier transforms are uncorrelated for different frequencies:

$$E \left[Y^*(f_1) Y(f_2) \right] = 0 \quad \text{for } f_1 \neq f_2 \quad 3.3.8$$

same as for stationary random processes.

Let us now assume that the random process with sample function $\beta(t)$ from eqn. 3.1.1 is of the type, where the averaging rule applied. We first write eqn. 3.1.1 in the form

$$\ddot{\beta} + (c_1 + a_1 \sin t) \dot{\beta} + (c_2 + a_2 \cos t) \beta = (c_3 + a_3 \sin t) \bar{\alpha} \quad 3.3.9$$

This equation is Fourier transformed by considering the following function pairs

$$\begin{aligned} \beta(t) &\longleftrightarrow B(f) \\ \cos t \beta(t) &\longleftrightarrow (1/2) \left\{ B(f - \frac{1}{2\pi}) + B(f + \frac{1}{2\pi}) \right\} \\ \dot{\beta}(t) &\longleftrightarrow 2\pi i f B(f) \\ \sin t \dot{\beta}(t) &\longleftrightarrow \pi \left\{ (f - \frac{1}{2\pi}) B(f - \frac{1}{2\pi}) - (f + \frac{1}{2\pi}) B(f + \frac{1}{2\pi}) \right\} \\ \ddot{\beta}(t) &\longleftrightarrow -(2\pi f)^2 B(f) \end{aligned} \quad 3.3.10$$

One then obtains

$$\begin{aligned} &-(2\pi f_1)^2 B(f_1) + c_1 2\pi i f_1 B(f_1) + a_1 \pi \left\{ (f_1 - \frac{1}{2\pi}) B(f_1 - \frac{1}{2\pi}) \right. \\ &\left. - (f_1 + \frac{1}{2\pi}) B(f_1 + \frac{1}{2\pi}) \right\} + c_2 B(f_1) + \frac{a_2}{2} \left\{ B(f_1 - \frac{1}{2\pi}) + B(f_1 + \frac{1}{2\pi}) \right\} = \\ &c_3 \bar{A}(f_1) + \frac{a_3}{2} \left\{ \bar{A}(f_1 - \frac{1}{2\pi}) + \bar{A}(f_1 + \frac{1}{2\pi}) \right\} \end{aligned} \quad 3.3.11$$

The conjugate complex equation with f_2 instead of f_1 reads:

$$\begin{aligned} & -(2\pi f_2)^2 B^*(f_2) - c_1 2\pi i f_2 B^*(f_2) + a_1 \pi \left\{ \left(f_2 - \frac{1}{2\pi}\right) B^*\left(f_2 - \frac{1}{2\pi}\right) \right. \\ & \left. - \left(f_2 + \frac{1}{2\pi}\right) B^*\left(f_2 + \frac{1}{2\pi}\right) \right\} + c_2 B^*(f_2) + \frac{a_2}{2} \left\{ B^*\left(f_2 - \frac{1}{2\pi}\right) + B^*\left(f_2 + \frac{1}{2\pi}\right) \right\} = \\ & c_3 \bar{A}^*(f_2) + \frac{a_3}{2} \left\{ \bar{A}^*\left(f_2 - \frac{1}{2\pi}\right) + \bar{A}^*\left(f_2 + \frac{1}{2\pi}\right) \right\} \end{aligned} \quad 3.3.12$$

Multiplying the last two equations with each other and taking the expectation of the product leads to an equation for the double frequency spectral density $S_\beta(f_1, f_2)$. Multiplying this equation further with $\delta(f_2 - f_1)$ reduces the double frequency spectra to single frequency spectra corresponding to the time averaged autocorrelation function. In this final equation the imaginary terms cancel each other:

$$\begin{aligned} & \bar{S}_\beta(f) \left\{ (2\pi f)^4 + (c_1 2\pi f)^2 - 2c_2 (2\pi f)^2 + c_2^2 \right\} \\ & + \bar{S}_\beta\left(f + \frac{1}{2\pi}\right) \left\{ \frac{a_1^2}{4} (2\pi(f + \frac{1}{2\pi}))^2 - \frac{a_1 a_2}{2} 2\pi(f + \frac{1}{2\pi}) + \frac{a_2^2}{4} \right\} \\ & + \bar{S}_\beta\left(f - \frac{1}{2\pi}\right) \left\{ \frac{a_1^2}{4} (2\pi(f - \frac{1}{2\pi}))^2 + \frac{a_1 a_2}{2} 2\pi(f - \frac{1}{2\pi}) + \frac{a_2^2}{4} \right\} \\ & = c_3^2 S_{\bar{\alpha}}(f) + \frac{a_3^2}{4} \left\{ S_{\bar{\alpha}}\left(f - \frac{1}{2\pi}\right) + S_{\bar{\alpha}}\left(f + \frac{1}{2\pi}\right) \right\} \end{aligned} \quad 3.3.13$$

We have here a functional equation between $S_{\bar{\alpha}}(f)$ and $\bar{S}_\beta(f)$ which can be approximated by a system of linear equations valid at the frequency points $0, \Delta f, 2\Delta f, \dots$. By inverting this system of linear equations $\bar{S}_\beta(f)$ can be obtained from $S_{\bar{\alpha}}(f)$. The details of the computation are presented in Appendix B.

Again, in the absence of a rigorous solution of the problem it is not possible to establish the advance ratio range for which eqn. 3.3.13 is useful. An attempt has been made to compare the result of eqn. 3.3.13 for a number of cases with the results of simulator studies. As of now, the comparison is not conclusive.

Numerical computations of $\bar{S}_\beta(f)$ in Appendix B, assuming a blade inertia number of $\gamma = 4$ and an advance ratio of $\mu = .3$ have shown, that for typical power spectral density distributions $S_{\bar{\alpha}}(f)$ equation 3.3.13 gives a blade flapping power spectral density $\bar{S}_\beta(f)$ which is approximately identical to that obtained with equation 3.2.3. It would then appear, that the damping and stiffness variation in eqn. 3.1.1 is negligible up to an advance ratio of $\mu = .3$. The reason for this result is that for $\gamma = 4$ and $\mu = .3$ the numerical values for a_1^2 , $a_1 a_2$ and a_2^2 are two orders of magnitude smaller than the numerical values for c_1 and c_2 .

4. Random Flap Bending

Though ultimately the problem of random blade flap bending will have to be solved for non stationary random inputs including the periodic parameter variations of the system, the analysis in this section ignores the non stationary character of the input and the time variability of the parameters. Nevertheless, the many degrees of freedom and the multiple correlated random inputs require a rather complex analysis. The usual variability of stiffness and mass over the blade length make a rigorous solution of the dynamic problem not feasible and numerical approximations must be developed. The method selected here makes use of influence coefficient and stiffness matrices derived from a certain discretization of the blade.

Three types of analysis are outlined. For the first type the system response is computed directly with the general admittance matrix. For the second type the response is computed with the help of the real normal modes of the undamped system. Under certain conditions normal mode cross damping terms are negligible and the admittance matrix is diagonalized. If these conditions are not satisfied a third type of analysis is possible where the second order differential equations with respect to time are transformed into a first order system. The eigenfunctions of this system are complex, but the admittance matrix can be diagonalized for this system without any limitations.

The discrete blade element considered in the present analysis is a simple one - a rigid element in which the bending stiffness is simulated by introducing torsional springs at the ends. The matrix formulation of the problem is not much more complicated if, instead, elastic elements with constant or linearly varying strains are used as suggested for example in Ref. (14).

4.1 Derivation of Blade Stiffness Matrix

In a rotating reference system the equation for the vertical deflections y (positive up) of a rotating blade in hovering, using quasistatic aerodynamics and neglecting coupling with chordwise bending and torsion reads (see for example Ref. (15))

$$(EIy'')'' - (Ty')' + m\ddot{y} + ac\rho \frac{\Omega r}{2} \dot{y} = \alpha ca\rho \frac{(\Omega r)^2}{2} y \quad 4.1.1$$

Instead of solving this differential equation by numerical methods the blade is subdivided into a number of rigid elements connected by torsion springs in the way shown in Fig. 1. Mass, aerodynamic damping, and imposed external forces are assumed to be concentrated at the element midpoint. In order to obtain the influence coefficient or stiffness matrix of the discretized blade, we assume forces F_n acting at the element midpoints and compute the vertical deflections y_n at these points from the equilibrium equations.

The horizontal force equilibrium equations

$$T_{n+1} + m_n x_n \Omega^2 - T_n = 0, \quad n = 1, 2, \dots, m \quad 4.1.2$$

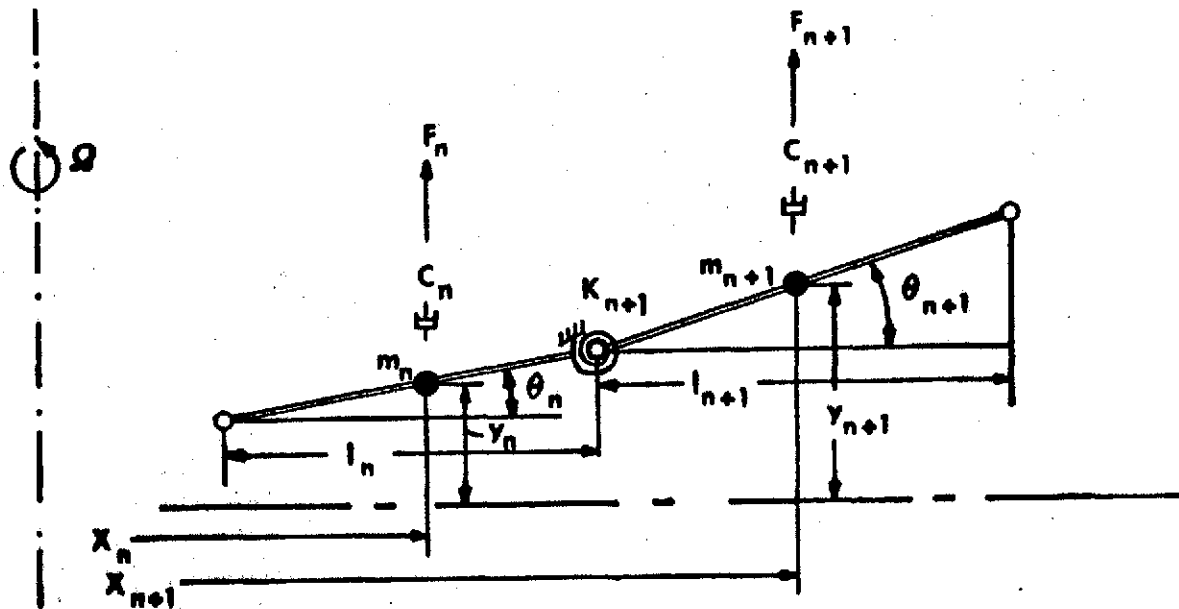
are uncoupled from the remaining blade equilibrium equations and can be summed to obtain the tension force T_n :

$$T_n = \sum_{p=n+1}^m \Omega^2 m_p x_p \quad 4.1.3$$

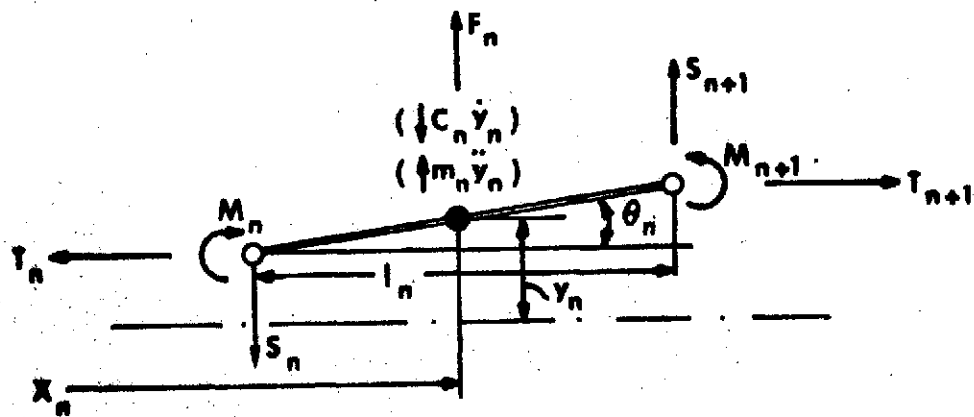
m designates the furthest out blade element at the blade tip.

The moment equilibrium about the left endpoint of element n is expressed by the equation

$$M_n - M_{n+1} + T_{n+1} \theta_n l_n = S_{n+1} l_n + F_n \frac{l_n}{2}, \quad 4.1.4$$



DIMENSIONS AND LOADING FOR ANY TWO ADJOINING ELEMENTS WITH LUMPED PARAMETERS OF MASS, DAMPING AND STIFFNESS.



FORCE SYSTEMS ON A TYPICAL ELEMENT n .
(DYNAMIC FORCES ARE SHOWN IN BRACKETS)

FIGURE 1 DISCRETE ELEMENT IDEALIZATION FOR BLADE FLAP-BENDING

or, introducing the shearforce

$$S_{n+1} = \sum_{j=n+1}^m F_j \quad 4.1.5$$

by the equation

$$M_n - M_{n+1} + T_{n+1} \theta_n \frac{l_n}{2} = l_n \sum_{j=n+1}^m F_j + F_n \frac{l_n}{2} \quad 4.1.6$$

There are m equations of this type

Introducing the spring constant of the torsion spring at the point $x_n + \frac{l_n}{2}$ by

$$K_{n+1} = \frac{EI_{n+1}}{x_{n+1} - x_n} \quad 4.1.7$$

the torsion spring equation reads

$$\theta_{n+1} - \theta_n = \frac{M_{n+1}}{K_{n+1}} \quad 4.1.8$$

For the cantilever blade there are m equations of this type.

For a hinged blade the first torsion spring equation is

replaced by the boundary condition $M_1 = 0$.

Finally the relation between slopes θ_n and vertical deflection y_n is obtained:

$$y_{n+1} - y_n = \theta_n \frac{l_n}{2} + \theta_{n+1} \frac{l_{n+1}}{2} \quad 4.1.9$$

There are m equations of this type, the first one having the form

$$y_1 = \theta_1 \frac{l_1}{2}$$

Thus the $3m$ unknowns $y_1 \dots y_m$, $\theta_1 \dots \theta_m$, $M_1 \dots M_m$ are uniquely defined by the $3m$ equations 4.1.6, 4.1.8 and 4.1.9. Since the last set of equations is independent of the first two sets,

$\theta_1 \dots \theta_m$, $M_1 \dots M_m$ are calculated from equations 4.1.6 and 4.1.8, while eqn. 4.1.9 is required for the calculation of the influence coefficients. Once the influence coefficient matrix $[w]$ with the elements

$$w_{jk} = \frac{y_j}{F_k}$$

has been computed, the stiffness matrix $[k]$ is obtained by inversion, since

$$[w] [k] = [I] \quad 4.1.10$$

4.2 Response Analysis with General Admittance Matrix

The equations of vertical motion for an assemblage of discrete blade elements have in matrix notation the form

$$[m] \{\ddot{y}\} + [c] \{\dot{y}\} + [k] \{y\} = \{f\} \quad 4.2.1$$

In subscript notation these equations read

$$m_k \ddot{y}_k + c_k \dot{y}_k + \sum_j k_{kj} y_j = f_k, \quad k = 1, \dots, m.$$

$[m]$, $[c]$ and $[k]$ are the mass, damping and stiffness matrices respectively. For the blade flap bending problem mass and damping matrices are diagonal, however, the theory is developed here for the general case of non diagonal mass and damping matrices. Various aspects of the response analysis of linear systems under random excitations are presented in References (8), (9), (10), (16), (17). The common features in all these investigations are the following:

- 1) discretize the continuum to obtain a tractable spectral representation of the exciting system of random loads in different elements by different correlated random processes.
- ii) under the hypothesis of weakly stationary and ergodic behaviour of the random process determine the output power spectral densities from admittance matrix and input power spectral densities.

The complex admittance matrix for the system defined by equation 4.2.1 is

$$[H(\omega)] = [-\omega^2 [m] + i\omega [c] + [k]]^{-1} \quad 4.2.2$$

This expression replaces the frequency response function given in eqn. 3.2.2 for blade flapping. ω has been substituted for $2\pi f$. The complex natural frequencies are obtained as the roots of the characteristic equation

$$|\lambda^2 [m] + \lambda [c] + [k]| = 0 \quad 4.2.3$$

Under weakly stationary and ergodic assumptions, the input power spectral density and the admittance matrix completely describe the output power spectral density. The power spectral densities now occur in form of matrices. For example the matrix $[S^f(\omega)]$ with elements $S_{jk}^f(\omega)$ is defined by

$$S_{jk}^f(\omega) = E [F_j^*(\omega) F_k(\omega)] \quad 4.2.4$$

where $F_j(\omega)$ is the sample Fourier transform of the input random force acting on blade element j . The deflection or output power spectral density matrix $[S^y(\omega)]$ with elements $S_{jk}^y(\omega)$ is determined by

$$[S^y(\omega)] = [H^*(\omega)]^T [S^f(\omega)] [H(\omega)] \quad 4.2.5$$

This relation replaces eqn. 2.2.5 for a single degree of freedom system for which the output power spectral density equals the input power spectral density multiplied by the square of the frequency response function.

The autocorrelation functions of the single degree of freedom system is now also replaced by a matrix. For the input forces we have the cross-correlation matrix $[R^f(\tau)]$ with the elements $R_{jk}^f(\tau)$ defined by

$$R_{jk}^f(\tau) = E [f_j(t)f_k(t+\tau)] \quad 4.2.6$$

For $\tau = 0$ one obtains the force cross-correlation matrix between blade elements

$$[R^f(0)] = \int_{-\infty}^{\infty} [S^f(\omega)] d\omega \quad 4.2.7$$

and a similar expression for the deflection cross-correlation matrix

$$[R^y(0)] = \int_{-\infty}^{\infty} [S^y(\omega)] d\omega \quad 4.2.8$$

This expression replaces eqn. 2.2.6 for a single degree of freedom. The diagonal terms of $[R^y(0)]$ represent the mean square deflections of the various blade elements and the off-diagonal terms represent the deflection cross correlations between different blade elements.

In principle, given the input power spectral density matrix $[S^f(\omega)]$ and the complex admittance matrix $[H(\omega)]$, the output power spectral density matrix $[S^y(\omega)]$ can be computed from eqn. 4.2.5. It is noteworthy that this analysis can be performed without making any assumptions with respect to the damping matrix. But a major drawback is the manipulation of the admittance matrix containing complex elements. These difficulties are avoided in a modal analysis for which the admittance matrix is diagonalized.

4.3 Real Normal Mode Analysis

For many structural problems it is adequate to perform a normal mode analysis with the modes of the undamped system. If the damping is distributed in a certain way, or if normal mode cross damping terms can be neglected, one obtains in such a normal mode analysis uncoupled differential equations for the normal coordinates. Eqn. 4.2.1 can be easily transformed in such a way that the factor $[m]$ in the first term is replaced by the unit matrix $[I]$. With the definitions

$$\begin{aligned} \{\bar{y}\} &= [m]^{\frac{1}{2}} \{y\} \quad ; \quad \{\bar{f}\} = [m]^{-\frac{1}{2}} \{f\} \\ [\bar{c}] &= [m]^{-\frac{1}{2}} [c] [m]^{-\frac{1}{2}} \quad ; \quad [\bar{k}] = [m]^{-\frac{1}{2}} [k] [m]^{-\frac{1}{2}} \end{aligned}$$

and omitting the bars over all symbols Eqn. 4.2.1 is obtained in the form

$$\{\ddot{y}\} + [c] \{\dot{y}\} + [k] \{y\} = \{f\} \quad 4.3.1$$

where $[c]$ and $[k]$ are symmetrical matrices. The normal modes of the undamped system are obtained from

$$[A] [\omega^2] = [k] [A] \quad 4.3.2$$

$[A]$ is the modal matrix with elements $A_{j\nu}$, where the latin subscript refers to the element number and the greek subscript to the mode number. The modal matrix $[A]$ can be multiplied by an arbitrary diagonal matrix and the product would still satisfy Eqn. 4.3.2. From the symmetry of $[k]$ it follows that both $[A]^T [A]$ and $[A]^T [k] [A]$ are diagonal matrices. Selecting a suitable normalization for $[A]$ one can obtain

$$[A]^T [A] = [I] \quad , \quad 4.3.3$$

$$[A]^T [k] [A] = [\omega^2] \quad 4.3.4$$

From 4.3.3:

$$[A]^{-1} = [A]^T \quad 4.3.5$$

The inverse modal matrix equals the transposed modal matrix.
Equations 4.3.2 and 4.3.4 read in subscript notation

$$A_{j\nu} \omega_\nu^2 = \sum_i k_{ji} A_{i\nu} \quad 4.3.6$$

$$\omega_\nu^2 = \chi_\nu \quad 4.3.7$$

$$\text{where } \chi_\nu = \sum_{ji} A_{j\nu} k_{ji} A_{i\nu} \quad 4.3.8$$

is an element of the diagonalized stiffness matrix.

If all natural frequencies ω_ν are different, the modal columns $A_{j\nu}$ form a system of linearly independent vectors and the expansion theorem holds, for example

$$\{y\} = [A]\{\eta\} \quad \text{or} \quad y_j = \sum_\nu A_{j\nu} \eta_\nu \quad 4.3.9$$

The η_ν are the modal deflections.

Inserting Eqn. 4.3.8 in Eqn. 4.3.1 and premultiplying by $[A]^T$ one obtains

$$[A]^T [A] \{\ddot{\eta}\} + [A]^T [c] [A] \{\dot{\eta}\} + [A]^T [k] [A] \{\eta\} = [A]^T \{f\} \quad 4.3.10$$

Because of Eqn. 4.3.3 and 4.3.4 this reduces to

$$\{\ddot{\eta}\} + [A]^T [c] [A] \{\dot{\eta}\} + [\omega^2] \{\eta\} = \{\varphi\} \quad 4.3.11$$

where the modal force column $\{\varphi\}$ is given by

$$\{\varphi\} = [A]^T \{f\} \quad \text{or} \quad \varphi_\nu = \sum_j A_{j\nu} f_j \quad 4.3.12$$

In general the modal equations 4.3.10 are coupled by the cross damping terms. Only if $[c]$ is of the form

$$[c] = a + b [k] \quad 4.3.13$$

with arbitrary constants a and b is the triple product in Eqn. 4.3.10, because of Eqns. 4.3.3 and 4.3.4, a diagonal matrix. In this case one can write

$$[A]^T [c] [A] = 2 [\omega] [\zeta]$$

and Eqn. 4.3.10 becomes

$$\{\ddot{\eta}\} + 2 [\omega] [\zeta] \{\dot{\eta}\} + [\omega] \{\eta\} = \{\varphi\} \quad 4.3.14$$

$$\text{or} \quad \ddot{\eta}_\nu + 2\omega_\nu \zeta_\nu \dot{\eta}_\nu + \omega_\nu^2 \eta_\nu = \varphi_\nu \quad 4.3.15$$

If Eqn. 4.3.12 is not satisfied and if the damping is small, the off-diagonal terms of the triple product $[A]^T [c] [A]$ are often neglected and the uncoupled equations 4.3.15 are used.

The modal frequency response function for the ν th mode is according to Eqn. 4.3.15

$$H_\nu(\omega) = \frac{1}{\omega_\nu^2 \left(1 - \left(\frac{\omega}{\omega_\nu} \right)^2 + 2i\zeta_\nu \frac{\omega}{\omega_\nu} \right)} \quad 4.3.16$$

$$\text{so that} \quad \{\eta\} = [H_\nu(\omega)] \{\varphi\} \quad 4.3.17$$

Inserting $\{\eta\}$ in Eqn. 4.3.9 and considering Eqn. 4.3.12 one obtains

$$\{y\} = [A] [H_\nu(\omega)] [A]^T \{f\} \quad 4.3.18$$

The general admittance matrix for Eqn. 4.3.1 defined by

$$[H(\omega)] = \left[-\omega^2 [I] + i\omega [c] + [k] \right]^{-1}$$

is therefore obtained from the diagonal modal admittance matrix $[H_\nu(\omega)]$ by

$$[H(\omega)] = [A] [H_\nu(\omega)] [A]^T \quad 4.3.19$$

$$\text{or} \quad H_{ij}(\omega) = \sum_\nu A_{i\nu} H_\nu(\omega) A_{j\nu}$$

For a probabilistic description of the response of discrete systems to random excitation, using real normal modes, the cross correlations and cross power spectral densities must be expressed in terms of normal coordinates. We then have to distinguish between the following cross correlation functions: (As before, it is assumed that all mean values are zero)

$$\text{Local force correlation} \quad R_{jk}^f(\tau) = E \left[f_j^*(t) f_k(t+\tau) \right] \quad 4.3.20$$

$$\text{Local deflection correlation} \quad R_{jk}^y(\tau) = E \left[y_j^*(t) y_k(t+\tau) \right] \quad 4.3.21$$

$$\text{Modal force correlation} \quad R_{\nu\mu}^\varphi(\tau) = E \left[\varphi_\nu^*(t) \varphi_\mu(t+\tau) \right] \quad 4.3.22$$

$$\text{Modal deflection correlation} \quad R_{\nu\mu}^\eta(\tau) = E \left[\eta_\nu^*(t) \eta_\mu(t+\tau) \right] \quad 4.3.23$$

In matrix notation these 4 functions are written respectively

$$\left[R^f(\tau) \right], \left[R^y(\tau) \right], \left[R^\varphi(\tau) \right], \left[R^\eta(\tau) \right]$$

Physical forces and deflections are, of course, real quantities. However, in the next section a description will be given which admits complex coordinates. For this reason the preceding definitions have been formulated in such a way that they also apply to complex force and deflection coordinates.

Inserting eqn. 4.3.9 in eqn. 4.3.21 one obtains with eqn. 4.3.23

$$R_{jk}^y = \sum_{\nu\mu} A_{j\nu}^* R_{\nu\mu}^\eta A_{k\mu} \quad 4.3.24$$

or $\left[R^y \right] = \left[A^* \right] \left[R^\eta \right] \left[A \right]^T$

This is a relation between modal and local cross correlation matrix. Eqn. 4.3.24 can be easily inverted because of

$$\left[A \right]^T \left[A \right] = \left[I \right] \text{ and one obtains} \quad \left[R^\eta \right] = \left[A^* \right]^T \left[R^y \right] \left[A \right] \quad 4.3.25$$

Similar relations exist for the force correlation matrices:

$$\begin{bmatrix} R^f \end{bmatrix} = \begin{bmatrix} A^* \end{bmatrix} \begin{bmatrix} R^\varphi \end{bmatrix} \begin{bmatrix} A \end{bmatrix}^T \quad 4.3.26$$

$$\begin{bmatrix} R^\varphi \end{bmatrix} = \begin{bmatrix} A^* \end{bmatrix}^T \begin{bmatrix} R^f \end{bmatrix} \begin{bmatrix} A \end{bmatrix} \quad 4.3.27$$

The cross spectra are obtained from the cross correlations by

$$S_{jk}^y(\omega) = \frac{1}{2\pi} \int_{-\infty}^{\infty} e^{-i\omega\tau} R_{jk}^y(\tau) d\tau \quad 4.3.28$$

with the inverse

$$R_{jk}^y(\tau) = \int_{-\infty}^{\infty} e^{i\omega\tau} S_{jk}^y(\omega) d\omega \quad 4.3.29$$

Therefore, the transformations 4.3.24 and 4.3.25 are also valid for the cross spectra:

$$\begin{bmatrix} S^y \end{bmatrix} = \begin{bmatrix} A^* \end{bmatrix} \begin{bmatrix} S^\eta \end{bmatrix} \begin{bmatrix} A \end{bmatrix}^T \quad 4.3.30$$

$$\begin{bmatrix} S^\eta \end{bmatrix} = \begin{bmatrix} A^* \end{bmatrix}^T \begin{bmatrix} S^y \end{bmatrix} \begin{bmatrix} A \end{bmatrix} \quad 4.3.31$$

Similar relations exist for the force spectra:

$$\begin{bmatrix} S^f \end{bmatrix} = \begin{bmatrix} A^* \end{bmatrix} \begin{bmatrix} S^\varphi \end{bmatrix} \begin{bmatrix} A \end{bmatrix}^T \quad 4.3.32$$

$$\begin{bmatrix} S^\varphi \end{bmatrix} = \begin{bmatrix} A^* \end{bmatrix}^T \begin{bmatrix} S^f \end{bmatrix} \begin{bmatrix} A \end{bmatrix} \quad 4.3.33$$

The modal frequency response function 4.3.16 now relates the modal force and modal deflection spectra:

$$S_{\nu\mu}^\eta(\omega) = H_{\nu}^*(\omega) S_{\nu\mu}^\varphi(\omega) H_{\mu}(\omega) \quad 4.3.34$$

a relation which is obtained from eqn. 4.2.5 by premultiplication with $\begin{bmatrix} A^* \end{bmatrix}^T$ and post multiplication with $\begin{bmatrix} A \end{bmatrix}$ and by considering

eqns. 4.3.19, 4.3.31 and 4.3.33. Rather than manipulating the complex admittance matrix $[H(\omega)]$ used in eqn. 4.2.5, the normal mode analysis allows a very simple computation of response spectra from input spectra according to eqn. 4.3.34. If the local force spectra are given and the local deflection spectra are desired, it is necessary to first transform the local force spectra to modal force spectra with the help of eqn. 4.3.33, and then to transform the modal deflection spectra to local deflection spectra with the help of eqn. 4.3.30.

Finally the local cross correlation matrix is calculated from eqn. 3.5.8 for $\tau = 0$:

$$R_{jk}^y(0) = \int_{-\infty}^{\infty} S_{jk}^y(\omega) d\omega \quad 4.3.35$$

The diagonal terms of this matrix are the mean square deflections of the blade elements. It should be once more pointed out that the real normal mode analysis is only applicable if either the damping matrix has the form given in eqn. 4.3.13 or if the cross damping terms in the modal equations 4.3.11 can be neglected.

4.4 Complex Normal Mode Analysis

For blade flap bending the conditions for the validity of the real normal mode analysis are not well satisfied, since the damping matrix is neither proportional to the mass or stiffness matrix nor are the cross damping terms in the modal representation negligibly small. A rigorous normal mode analysis without neglecting terms is possible if one converts the m second order differential equations with respect to time into $2m$ first order equations equivalent to Hamilton's canonical equations. The new system of equations has $2m$ complex eigenvalues and $2n$ complex eigencolumns, if one excludes the case of multiple eigenvalues. It is further assumed, that the system is stable, though unstable systems can also be treated with this method if another coordinate transformation is performed, see Ref. (18). The inconvenience

of complex eigencolumns and complex normal coordinates in this method is in part compensated by the very simple form of the frequency response function.

With the transformation

$$\{\bar{y}\} = \begin{Bmatrix} \{\dot{y}\} \\ \{y\} \end{Bmatrix} \quad \text{for deflections} \quad 4.4.1$$

$$\{\bar{f}\} = \begin{Bmatrix} \{o\} \\ \{f\} \end{Bmatrix} \quad \text{for forces} \quad 4.4.2$$

equation 4.2.1 assumes the form

$$[M] \{\bar{y}\} + [K] \{\bar{y}\} = \{\bar{f}\} \quad 4.4.3$$

where

$$[M] = \begin{bmatrix} [O] & [m] \\ [m] & [c] \end{bmatrix} \quad 4.4.4$$

$$[K] = \begin{bmatrix} -[m] & [O] \\ [O] & [k] \end{bmatrix} \quad 4.4.5$$

The eigenvalue problem for eqn. 4.4.3 is defined by

$$[M] [\bar{A}] [\lambda] + [K] [\bar{A}] = 0 \quad 4.4.6$$

where $[\bar{A}]$ is the modal matrix. Eqn. 4.4.6 is the same as eqn. 4.3.1 except for the sign. From the symmetry of the matrices $[M]$ and $[K]$ one can derive the orthogonality relations

$$[\bar{A}]^T [M] [\bar{A}] = [\mu] \quad 4.4.7$$

$$[\bar{A}]^T [K] [\bar{A}] = [\kappa] \quad 4.4.8$$

If all eigenvalues λ_ν are different the complex eigenvectors $\bar{A}_{j\nu}$ form a system of linearly independent vectors and the expansion theorem holds:

$$\bar{y}_j = \sum_\nu \bar{A}_{j\nu} \bar{\eta}_\nu, \text{ or } \{\bar{y}\} = [\bar{A}]\{\bar{\eta}\} \quad 4.4.9$$

Inserting this sum into eqn. 4.4.3 and premultiplying by $[\bar{A}]^T$ one obtains with eqns. 4.4.7 and 4.4.8:

$$[\mu]\{\bar{\eta}\} + [x]\{\bar{\eta}\} = \{\bar{\varphi}\} \quad 4.4.10$$

where $\{\bar{\varphi}\} = [\bar{A}]^T \{\bar{f}\} \text{ or } \bar{\varphi}_\nu = \sum_j \bar{A}_{j\nu} \bar{f}_j \quad 4.4.11$

With

$$[x][\mu]^{-1} = -[\lambda] \quad 4.4.12$$

one can write the set of $2m$ uncoupled equations 4.4.10 in the form

$$\{\dot{\bar{\eta}}\} - [\lambda]\{\bar{\eta}\} = [\bar{\varphi}][\mu]^{-1}$$

or

$$\dot{\bar{\eta}}_\nu - \lambda_\nu \bar{\eta}_\nu = \bar{\varphi}_\nu / \mu_\nu \quad 4.4.13$$

Eqn. 4.4.13 has the modal frequency response function

$$\bar{H}_\nu(\omega) = \frac{1}{(i\omega - \lambda_\nu)\mu_\nu} \quad 4.4.14$$

Formally all relations of section 4.3 are still valid if y and η are replaced by \bar{y} and $\bar{\eta}$ and f and φ are replaced by \bar{f} and $\bar{\varphi}$ respectively. While in section 4.3 the stars on $[A]$ were meaningless since $[A]$ was real, the complex character of $[\bar{A}]$ must now be properly considered.

Given the local force spectra $[S^f(\omega)]$ one first transforms to modal force spectra by

$$[S^{\bar{f}}(\omega)] = [\bar{A}^*]^T [S^f(\omega)] [\bar{A}], \quad 4.4.15$$

then to modal deflection spectra by

$$S_{\nu\mu}^{\bar{\eta}}(\omega) = \bar{H}_{\nu}^*(\omega) S_{\nu\mu}^{\bar{f}}(\omega) \bar{H}_{\mu}(\omega)$$

or

$$S_{\nu\mu}^{\bar{\eta}}(\omega) = \frac{S_{\nu\mu}^{\bar{f}}(\omega)}{\mu_{\nu}(i\omega - \lambda_{\nu})^* \mu_{\mu}(i\omega - \lambda_{\mu})} \quad 4.4.16$$

and finally to local deflection spectra by

$$[S^{\bar{y}}(\omega)] = [\bar{A}^*] [S^{\bar{\eta}}(\omega)] [\bar{A}]^T \quad 4.4.17$$

The transformation of the physical spectra $[S^y(\omega)]$ and $[S^f(\omega)]$ to the values for the first order system $[S^{\bar{y}}(\omega)]$ and $[S^{\bar{f}}(\omega)]$ are to be performed in agreement with equations 4.4.1 and 4.4.2.

$$\text{Since } S_{jk}^y(\omega) = E [Y_j^*(\omega) Y_k(\omega)]$$

one obtains from eqns. 4.4.1 and 4.4.2:

$$[S^{\bar{y}}(\omega)] = \left[\begin{array}{c|c} \omega^2 [S^y(\omega)] & i\omega [S^y(\omega)] \\ \hline -i\omega [S^y(\omega)] & [S^y(\omega)] \end{array} \right] \quad 4.4.18$$

$$[S^{\bar{f}}(\omega)] = \left[\begin{array}{c|c} [0] & [0] \\ \hline [0] & [S^f(\omega)] \end{array} \right] \quad 4.4.19$$

If $[S^y(\omega)]$ is given as the result of the modal analysis, it is easy to obtain $[S^y(\omega)]$ from eqn. 4.4.18. In Appendix C an algorithm is developed for the complex normal mode analysis of randomly excited multi-degree of freedom systems.

If $[S]$ is the stress-deflection matrix with matrix element S_{kj}^y (σ_k indicating the bending stress at blade station k) the physical stress cross correlation matrix is given by

$$[R^\sigma] = [S] [R^y] [S^*]^T \quad 4.4.20$$

5. Outline for Lifting Rotor Model Tests in Turbulent Flow

In the random blade flapping and blade flap bending theories presented in Sections 3 and 4, it is assumed that the random blade loads at the various blade stations are known, so that the output random flapping angles or flap bending deflections or moments can be computed. In the following, two types of model tests are outlined which have two different relations to the theory. In the first and more sophisticated type of model tests, the test results are used to substantiate the theory. In the second less sophisticated type of model tests the theory is required to interpret the test results. In both types of model tests information is obtained about the aerodynamic blade loads when the model is operated in a turbulent flow.

5.1 Model Tests with Both Load and Load Response Measurements

In order to substantiate the theory by experiments, it is required to record on tape at a number of blade stations the aerodynamic blade loads together with flapping angle (if flapping hinges are provided) and flap-bending strains. The tape recordings must be of sufficient length to allow adequate random data processing, say 500 rotor revolutions. The pressure pick-ups must be fast responding and the slip rings should not introduce excessive noise. Probably it will not be possible to install a sufficient number of pressure pick-ups to reliably integrate the blade aerodynamic loads, and it will be necessary to calculate the loads from the readings of a few strategically located pick-ups, possibly just from two pick-ups per blade station installed in the region of maximum pressure at the upper and lower airfoil surface. This system needs calibration in a flow of known fluctuations of the flow direction and of known overall aerodynamic pressures, which in itself will present problems. In addition to the model rotor instrumentation the turbulence characteristics of the inflow must be measured upstream of the model rotor, for example with a number of crossed hot wire probes.

These tests will require considerable preparation, but they should be valuable in obtaining data on both the aerodynamic loads and on the load responses of lifting rotors operating in turbulent flow, thus making a substantiation of the theory of Sections 3 and 4 possible.

5.2 Model Tests with Load Response Measurements Only

A much simpler test set-up is obtained, if the aerodynamic load measurements are omitted. In this case, only flapping angles and flap-bending strains would be recorded at a number of blade stations. The theory would then be used in order to establish the random aerodynamic load characteristics from the random response measurements. Same as in the previous case, the turbulence characteristics of the inflow must be measured upstream of the model rotor. These tests would not be a check of the theory which has to be assumed as valid, but the tests would be valuable in obtaining data on the random aerodynamic blade loads produced by the turbulent inflow. Depending on the character of this turbulence it might be possible to predict theoretically the rotor blade angle of attack fluctuations and thereby the blade load fluctuations from a given turbulence spectrum of the inflow. Most likely, however, the relation between inflow turbulence and the turbulence which the rotary wing feels will be a rather complex one and may not be easily tractable by a theoretical approach.

At Ames Research Center there is available a 4-bladed 12 ft. diameter propeller which could be used as generator for a turbulent flow by setting the two blade pairs at largely different incidence angles. Also available is a two bladed see-saw rotor of 9 ft. diameter which could be operated in the wake of the 4-bladed propeller.

A Minimum Instrumentation for the test is considered as follows:

1. Flapping angle pick-up, probably best obtained with a strain gauged flexure which is loaded in blade flapping.

2. Two strain gauges near the blade root, one for each blade, measuring flap-bending strain. Possibly more flap-bending strain gauges along the blade radius.
3. Blade azimuth indicator.
4. Two crossed hot wire probes, located upstream of the rotor in the rotor plane with a lateral distance of about .7 rotor diameters between each other.

The readings of items 1 to 4 must be tape recorded. In addition, blade incidence and rotor shaft incidence must be known.

6. Conclusions

- 6.1 The concepts for a theoretical and experimental study of lifting rotor random loads and vibrations have been developed. Random lifting rotor loads occur not only during operation in atmospheric turbulence but also in a quiet atmosphere when there can be a self induced turbulence of the flow through the rotor plane as in vertical descent in the vortex state, or as in transition from hovering to forward flight.
- 6.2 A survey of random process theory has shown that very little prior work has been done in the area of non stationary random processes, in particular when the system parameters are time varying. The only type of non stationary random processes which are presently analytically manageable are modulated stationary random processes. Under the assumption that the random processes associated with lifting rotor operation are of this type, it has been shown that up to an advance ratio of $\mu = .3$ the effect of the time variability of the system parameters in blade flapping is quite small. If confirmed by experimental hardware or simulator results, this would greatly simplify lifting rotor random loads and vibrations analyses except for very high advance ratios.
- 6.3 A rather complete theory of random blade flap-bending has been presented under the usual assumptions of stationary and ergodic behaviour. While the theoretical concepts are available, the numerical analysis is quite extensive. No previous work exists which would indicate the validity of possible approximations like the neglect of cross damping terms in the modal representation, or the neglect of the cross correlations between blade elements or blade modes, or the less drastic neglect of the quad spectra between blade elements or blade modes. A systematic computational and experimental approach to these important questions will be required. It is reassuring, however, that a complete cross correlation analysis is available

in principle and may well be computationally tractable.

- 6.4 Experimental work with lifting rotor models is proposed to study the random loads and load responses when the model is operating in a turbulent flow. With a rather sophisticated rotor model instrumented for the recording of both aerodynamic blade loads and blade responses to these loads, the theory could be substantiated. However, valuable test results can also be expected from a simple rotor model instrumented only for the recording of flapping angles and flap-bending strains. In such tests the theory would be required to interpret the test results with respect to random air loads produced by operation of the model rotor in turbulent flow.

References

1. Houbolt, J. C. Steiner, R. and Pratt, K. G., "Dynamic Response of Airplanes to Atmospheric Turbulence Including Flight Data on Input and Response" NASA TR R-199, June, 1964
2. Dempster, J. B. and Bell, C. A., "Summary of Flight Load Environmental Data Taken on B-52 Fleet Aircraft" Journal of Aircraft, Vol. 2, p. 398, Sept.-Oct., 1965
3. Dalzek, J. F. and Associates, "Studies of the Structural Response of Simulated Helicopter Rotor Blades to Random Excitation", AROD Contract No. 375, Interim Reports I and II, Sept., 1965 and Sept., 1966
4. Gilman, J., Jr. and Bennett, R. M., "A Wind-Tunnel Technique for Measuring Frequency-Response Functions for Gust Load Analyses", Journal of Aircraft, Vol. 3, p. 535, Nov.-Dec., 1966
5. Yaggy, Paul F. and Mort, Kenneth W., "Wind-Tunnel Tests of Two VTOL Propellers in Descent", NASA TN D-1766, March, 1963
6. Cramer, Harald and Leadbetter, M. R., "Stationary and Related Stochastic Processes", John Wiley & Sons, 1967
7. Bendat, J. S. and Piersol, A. G., "Measurement and Analysis of Random Data", John Wiley & Sons, 1966
8. Meirovitch, Leonard, "Analytical Methods in Vibrations", The MacMillan Co., New York, 1967
9. Davis, R. E., "Random Pressure Excitation of Shells and Statistical Dependence Effect of Normal Mode Response", NASA-CR-311, Sept., 1965
10. Newsome, C. O., Fuller, J. R. and Sherrer, R. E., "A Finite Element Approach to the Analysis of Randomly Excited Complex Elastic Structures", presented at the AIAA/ASME 8th Structures Conference, Palm Springs, California, March, 1967
11. Caughey, T. K., "Non Stationary Random Inputs and Responses", Volume 2 of "Random Vibration", edited by S. H. Crandall, The M.I.T. Press, Cambridge, Mass., 1963

12. Piersol, A. G., "Spectral Analysis of Non Stationary Spacecraft Vibration Data", NASA CR-341, Nov., 1965
13. Hohenemser, K. H. and Heaton, P. W., Jr., "Aeroelastic Instability of Torsionally Rigid Helicopter Blades", Journal Amer. Helicopter Soc., Vol. 12, No. 2, April, 1967
14. Argyris, J. H., "Continua and Discontinua, an Apercu of Recent Developments on Matrix Displacement Methods", Conference on Matrix Methods and Structural Mechanics, Wright-Patterson Air Force Base, Oct., 1965
15. Houbolt, J. C., and Brooks, G. W., "Differential Equations of Motion for Combined Flapwise Bending, Chordwise Bending, and Torsion of Twisted Non Uniform Rotor Blades", NACA-TN-3905, Feb., 1957
16. Newsome, C. O., "Finite Element Method of Complex Structures under Random Excitation", M.S. Thesis, University of Washington, 1967
17. Schweiker, W. and Davis, R. E., "Response of Complex Shell Structures to Aerodynamic Noise", NASA-CR 450, April, 1966
18. Hasselmann, K., "Uber Zufallserregte Schwingungssysteme" ZAMM, Vol. 42, p. 465, 1962
19. User's Manual, Washington University Computation Center, Feb., 1966
20. Pennington, R. G., "Introductory Computer Methods and Numerical Analysis", The MacMillan Co., New York, 1966
21. Joseph, J. G., "Computer Methods in Solid Mechanics", The MacMillan Co., New York, 1965
22. IBM Application Program, System/360 Scientific Subroutine Package (360 A-CM-03X) Version II, Programmer's Manual

Appendix A: Time Averaged Autocorrelation Function and Associated Power Spectral Density of a Stationary Random Process Modulated by a Periodic Function

If $y(t)$ is the product of a stationary random function $x(t)$ and a deterministic periodic function $A(t)$ (modulated stationary random process), then the random process obtained by averaging the autocorrelation function

$$\lim_{T \rightarrow \infty} \frac{1}{T} \int_{-T/2}^{T/2} R_y(t, \tau) dt = \bar{R}_y(\tau) \quad A-1$$

is a stationary random process and has the measurable single frequency power spectral density, see Section 9.5.3 of Ref. (7).

$$\bar{S}_y(\omega) = \int_{-\infty}^{\infty} \bar{R}_y(\tau) e^{-i\omega\tau} d\tau \quad A-2$$

As $A(t)$ is periodic, it can be expressed in Fourier series

$$A(t) = \sum_{k=-\infty}^{\infty} c_k e^{ik\omega_0 t}$$

Setting

$$y(t) = x(t) \sum_{k=-\infty}^{\infty} c_k e^{ik\omega_0 t}$$

one obtains

$$\begin{aligned} R_y(t_1, t_2) &= E \left[x(t_1) x(t_2) \left\{ \sum_{k=-\infty}^{\infty} c_k e^{ik\omega_0 t_1} \right\} \left\{ \sum_{l=-\infty}^{\infty} c_l e^{il\omega_0 t_2} \right\} \right] \\ &= R_x(t_2 - t_1) \sum_{k=-\infty}^{\infty} \sum_{l=-\infty}^{\infty} c_k c_l e^{i\omega_0(k t_1 + l t_2)} \end{aligned}$$

Substitute $t_2 - t_1 = \tau$ and $\frac{t_1 + t_2}{2} = t$, to get

$$R_y(\tau, t) = R_x(\tau) \sum_{k=-\infty}^{\infty} \sum_{l=-\infty}^{\infty} c_k c_l e^{i\omega_0\{(k+l)t + (l-k)\tau/2\}}$$

While applying equation A-1, it is easy to verify that

$$\lim_{T \rightarrow \infty} \frac{1}{T} \left[\frac{e^{i\omega_0(k+1)T}}{i\omega_0(k+1)} \right]_{-1/2}^{1/2} \rightarrow 0 \quad \text{except for } k = 1 = 0 \\ \text{ \& } k = \pm 1$$

As l and k can take both positive and negative values $l-k$ can take values $2k$ and $-2k$.

Therefore,

$$\bar{R}_y(\tau) = R_x(\tau) \sum_{\substack{k=-\infty \\ k \neq 0}}^{\infty} c_k^2 e^{i\omega_0(\pm 2k)\tau/2} + c_0^2 R_x(\tau)$$

Applying equation A-2, one gets a measurable single frequency power spectral density

$$\bar{S}_y(\omega) = S_x(\omega) c_0^2 + \sum_{\substack{k=-\infty \\ k \neq 0}}^{\infty} c_k^2 \left\{ S_x(\omega + k\omega_0) + S_x(\omega - k\omega_0) \right\} \quad A-3$$

Another way of obtaining the same result is to multiply the double frequency spectrum corresponding to the sample function $x(t)A(t)$ by $\delta(\omega_2 - \omega_1)$. This is shown in the following derivation.

With

$$y(t) = x(t) \sum_{k=-\infty}^{\infty} c_k e^{ik\omega_0 t},$$

set

$$Y^*(\omega_1) = \int_{-\infty}^{\infty} x(t_1) \sum_{k=-\infty}^{\infty} c_k e^{ik\omega_0 t_1} e^{i\omega_1 t_1} dt_1$$

to obtain

$$Y^*(\omega_1) = c_0 X^*(\omega_1) + \sum_{\substack{k=-\infty \\ k \neq 0}}^{\infty} c_k^* \left[X^*(\omega_1 - k\omega_0) + X^*(\omega_1 + k\omega_0) \right]$$

and

$$Y(\omega_2) = c_0 X(\omega_2) + \sum_{\substack{k=-\infty \\ k \neq 0}}^{\infty} c_k \left[X(\omega_2 - k \omega_0) + X(\omega_2 + k \omega_0) \right]$$

The double frequency spectrum is defined by

$$S_y(\omega_1, \omega_2) = E \left[Y^*(\omega_1) Y(\omega_2) \right]$$

We now multiply this double frequency spectrum with $\delta(\omega_2 - \omega_1)$:

$$\begin{aligned} \delta(\omega_2 - \omega_1) S_y(\omega_1, \omega_2) &= \delta(\omega_2 - \omega_1) c_0^2 S_x\left(\frac{\omega_1 + \omega_2}{2}\right) \\ &+ \sum_{\substack{k=-\infty \\ k \neq 0}}^{\infty} c_k^2 \delta(\omega_2 - \omega_1) S_x\left(\frac{\omega_2 - 2k \omega_0 + \omega_1}{2}\right) \\ &+ \sum_{\substack{k=-\infty \\ k \neq 0}}^{\infty} c_k^2 \delta(\omega_2 - \omega_1) S_x\left(\frac{\omega_2 + 2k \omega_0 + \omega_1}{2}\right) \end{aligned}$$

A-4

and obtain the same equation as A-3.

Appendix B: Computation of Power Spectral Density for a Flapping Randomly Excited Blade

Equation B-1 represents a general type of linear, second order and non-homogeneous differential equation with constant and periodic coefficients, $\beta(t)$ and $\alpha(t)$ representing respectively the non stationary random response and the stationary random input.

$$\ddot{\beta} + \{c_1 + a_1 \sin(n\omega_0 t + \theta_1)\} \dot{\beta} + \{c_2 + a_2 \sin(n\omega_0 t + \theta_2)\} \beta = \{c_3 + a_3 \sin(n\omega_0 t + \theta_3)\} \alpha(t) \quad \text{B-1}$$

(Selecting a time unit for which the rotor angular velocity $n\omega_0 = 1$ and substituting $\theta_1 = 0$, $\theta_2 = \frac{\pi}{2}$, $\theta_3 = 0$, $c_1 = c_3 = \frac{\gamma}{8}$, $a_1 = a_2 = \frac{\gamma\mu}{6}$, $c_2 = 1$, and $a_3 = \frac{\gamma\mu}{3}$ in equation B-1, an approximate blade flapping differential equation valid up to about $\mu = 0.3$ advance ratio, is obtained. For details refer to Section 3.) With the operator f representing the Fourier integral transformation, let

$$f(\ddot{\beta}) = -\omega^2 B(\omega)$$

$$f[\{c_1 + a_1 \sin(n\omega_0 t + \theta_1)\} \dot{\beta}] = B_1(\omega)$$

$$f[\{c_2 + a_2 \sin(n\omega_0 t + \theta_2)\} \beta] = B_2(\omega) \quad \text{and}$$

$$f[\{c_3 + a_3 \sin(n\omega_0 t + \theta_3)\} \alpha] = B_3(\omega).$$

Apply the operator f to equation B-1 at frequencies ω_1 and ω_2 to yield

$$-\omega_1^2 B^*(\omega_1) + B_1^*(\omega_1) + B_2^*(\omega_1) = B_3^*(\omega_1)$$

$$\text{and } -\omega_2^2 B(\omega_2) + B_1(\omega_2) + B_2(\omega_2) = B_3(\omega_2).$$

Now, consider

$$E \left[B^*(\omega_1) B(\omega_2) \right]$$

along the line $\omega_1 = \omega_2 = \omega$, as explained in Appendix A and set

$$\delta(\omega_2 - \omega_1) E \left[B^*(\omega_1) B(\omega_2) \right] = \bar{S}_\beta(\omega).$$

After some algebra one obtains

$$\begin{aligned} & \left\{ \omega^4 + c_1^2 \omega^2 - 2c_2 \omega^2 + c_2^2 \right\} \bar{S}_\beta(\omega) + \left\{ \frac{a_1^2}{4} (\omega - n\omega_0)^2 - \frac{a_1 a_2}{2} (\omega - n\omega_0) \sin(\theta_1 - \theta_2) \right. \\ & \left. + \frac{a_2^2}{4} \right\} \bar{S}_\beta(\omega - n\omega_0) \\ & + \left\{ \frac{a_1^2}{4} (\omega + n\omega_0)^2 + \frac{a_1 a_2}{2} (\omega + n\omega_0) \sin(\theta_1 - \theta_2) + \frac{a_2^2}{4} \right\} \bar{S}_\beta(\omega + n\omega_0) \\ & = c_3^2 S_\alpha(\omega) + \frac{a_3^2}{4} \left\{ S_\alpha(\omega + n\omega_0) + S_\alpha(\omega - n\omega_0) \right\} \end{aligned} \quad B-2$$

With $\omega = k\omega_0$ where k is a discrete variable with values $k = 1, 2, \dots$ and ω_0 a fixed step size, eqn. B-2 represents an infinite set of difference equations for $\bar{S}_\beta(k\omega_0)$ which will be abbreviated by $S_k(\omega)$. Since $S_{k-n}(\omega) = S_{-k+n}(\omega)$ and since from physical considerations $S_{k+n}(\omega) \rightarrow 0$ for large k , the infinite set of equations can be approximated by a finite set.

Express equation B-2 in a symbolic form

$$A(k, k) S_k(\omega) + A(k-n, k) S_{k-n}(\omega) + A(k+n, k) S_{k+n}(\omega) = \text{R.H.S.} \quad B-3$$

Equation B-3 is inverted for $S_k(\omega)$ values by a digital computer program (19) which essentially involves a matrix inversion subroutine. Figures 2a-d show numerical results for two stochastic inputs $S_{\bar{\alpha}}(\omega)$. Figures 2a and 2b with $a_1 = a_2 = .2$ refer to an advance ratio $\mu = 0.3$ and a blade inertia number $\gamma = 4$. For this set of coefficients the values $A(k-n, k)$ and $A(k+n, k)$ are two order of magnitude smaller than $A(k, k)$ which explains the fact that the results of the present algorithm do not differ appreciably from those for the constant parameter system

obtained by omitting the periodic terms in eqn. B-1. The results obtained for the same set of stochastic inputs but now with $a_1 = a_2 = 0.8$ show a substantial difference, Figures 2c and 2d, between the present method and the equivalent constant parameter system, as expected. It is to be noted that the second set of coefficients have no physical relevance as the approximate blade flapping equation is valid up to about $\mu = 0.3$ advance ratio and the blade inertia number is generally less than 10 for helicopters.

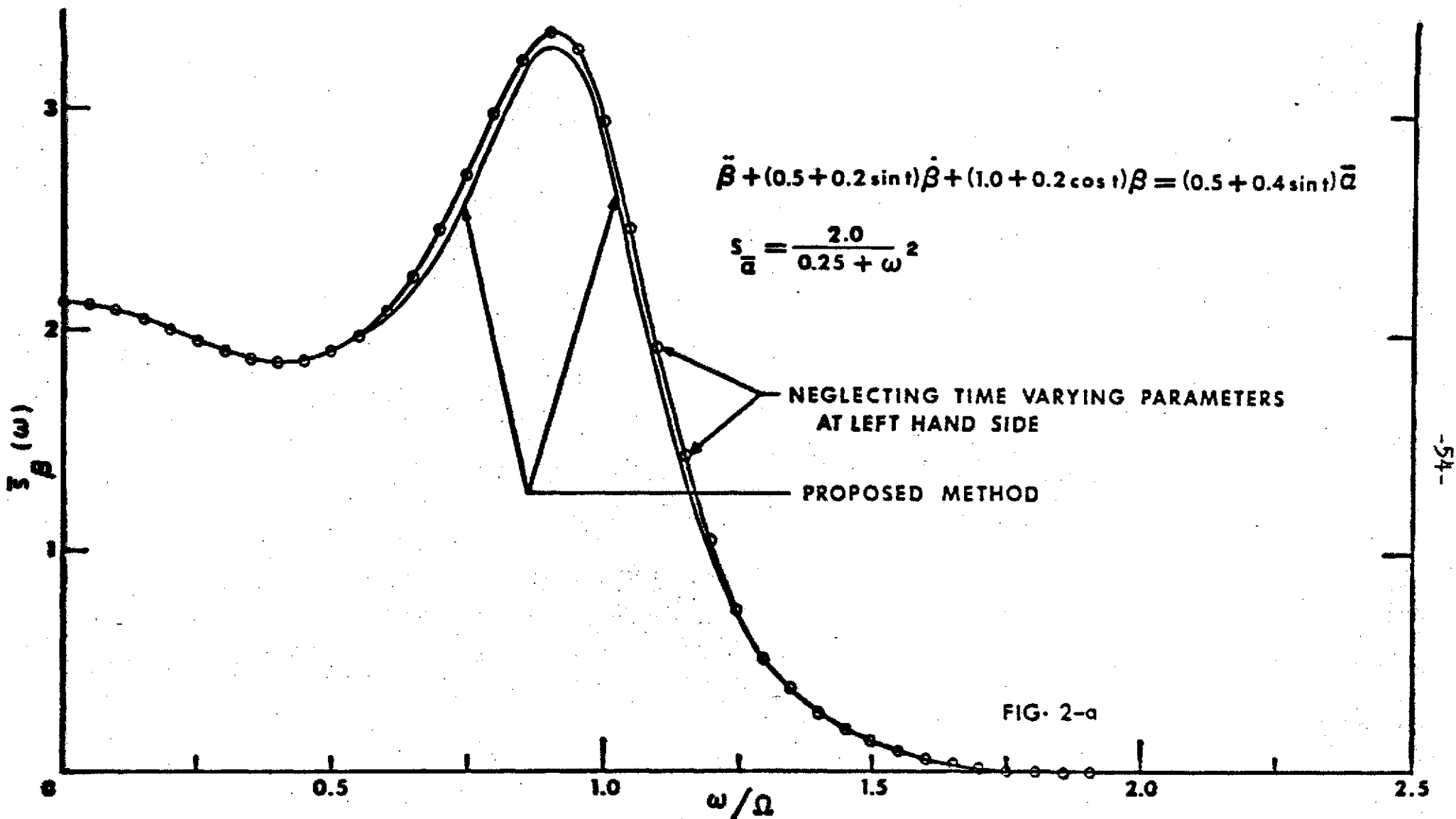
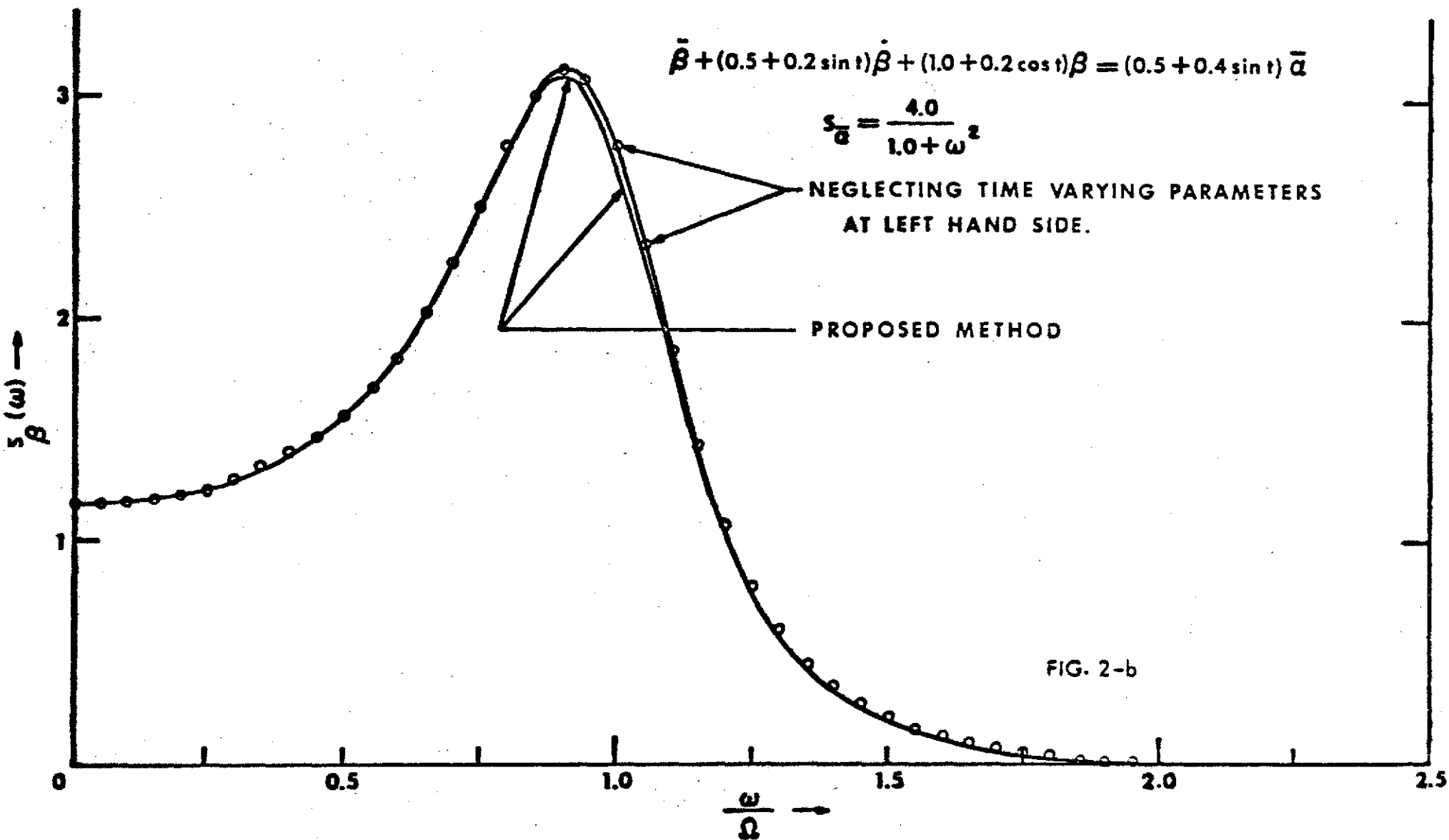
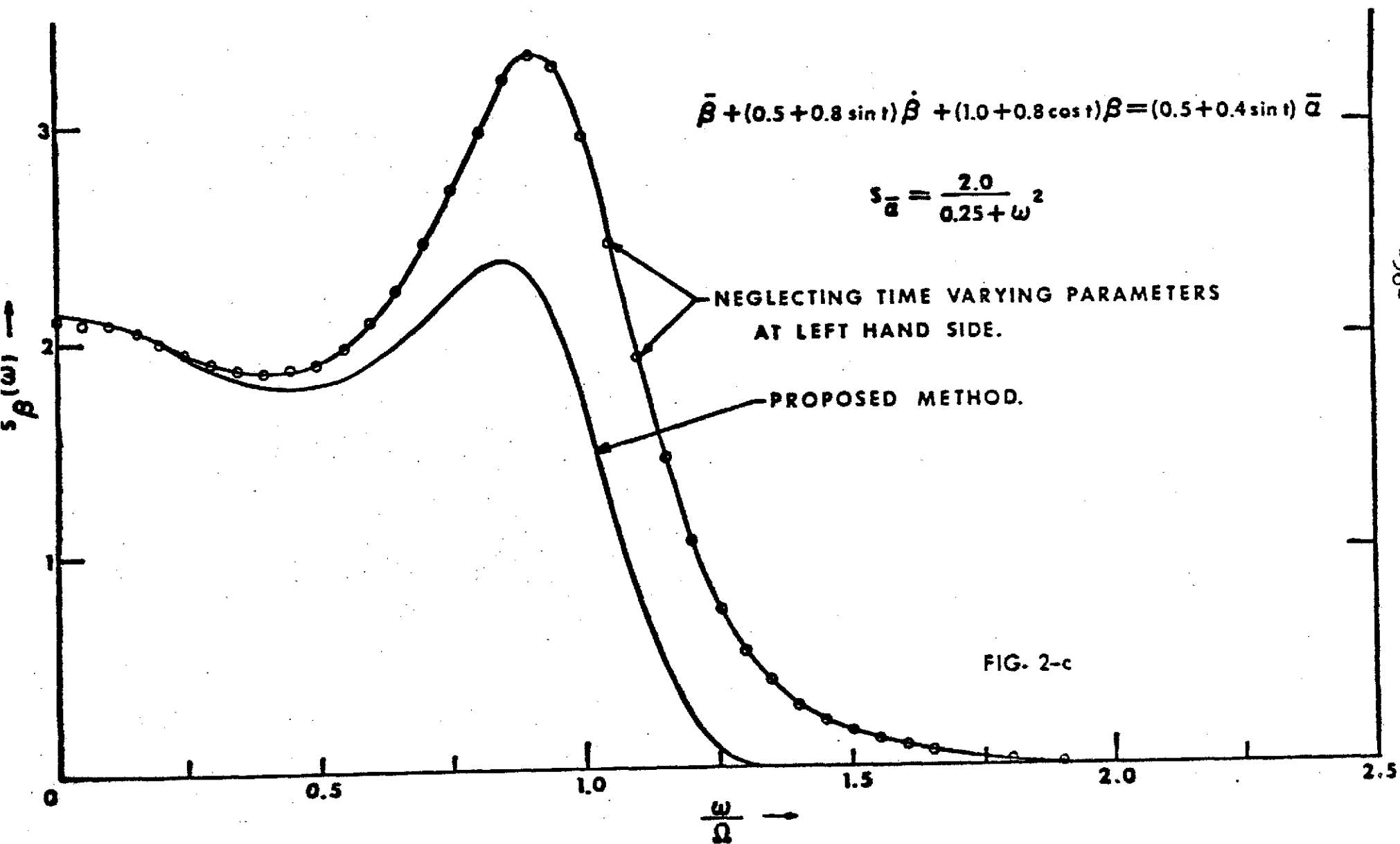
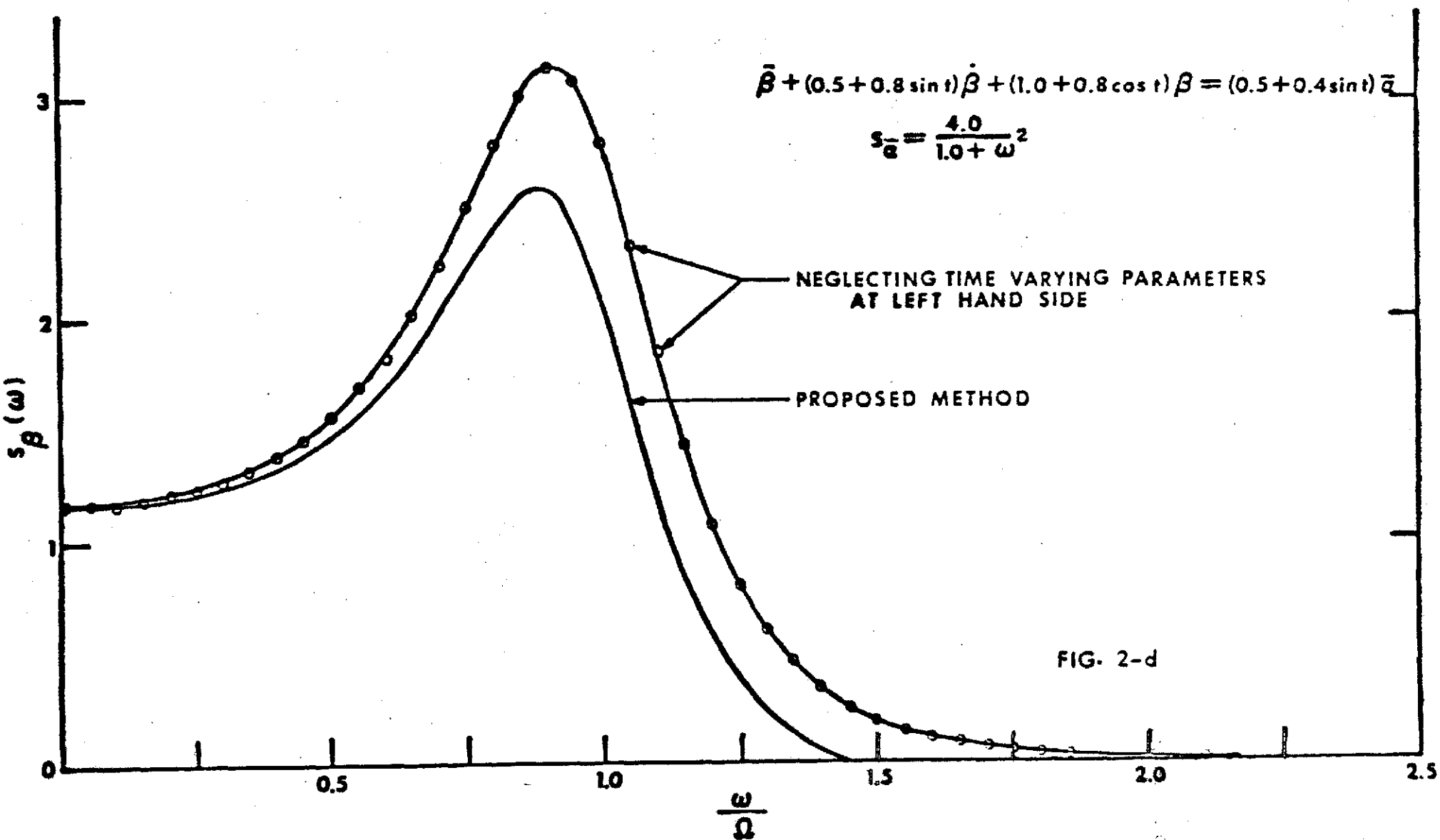


FIGURE 2:- SPECTRAL DENSITY OF FLAPPING OSCILLATIONS OF RIGID BLADES IN FORWARD HELICOPTER FLIGHT, ASSUMING THE RESPONSE TO BE A STATIONARY RANDOM PROCESS MODULATED BY PERIODIC FUNCTIONS. (Equations given above represent the corresponding blade flapping equation and the assumed spectral density of the mean blade angle of attack $\bar{\alpha}$ respectively.)







Appendix C: Discrete Element Algorithm for Complex Normal Mode Analysis of Multi Degree of Freedom Stable Systems Under Random Excitation

Before actually coming to the numerical analysis, it is mandatory to replace the continuum as an assemblage of 'm' discrete elements to obtain 'm' equations of dynamic equilibrium in a standard form, equation 4.2.1, and then, as discussed in Section 4.4, convert these m equations into 2m first order differential equations having 2m complex eigenvalues and 2m complex modal columns. The discussion here is restricted to blade flap-bending random analysis with small advance ratio though the present algorithm is applicable to any discrete systems under random excitation.

The analysis of numerical problems comprises three main phases:

- 1) the mass, damping and stiffness matrices
- 2) the eigenvalues and eigencolumns
- 3) the spectral density matrices and RMS deflection and stress values at element stations. The numerical operations are carried out in two passes - the first two phases in the first run and the last one in the second run.

The computer program, written in FORTRAN IV language is based on some of the subroutines appearing elsewhere in the literature (19, 20, 21, 22). It accepts as inputs the following information regarding the pattern of discretization and other constants associated with the physical system.

- i) number of elements
- ii) Hubradius
- iii) boundary conditions at the hubjoint
- iv) lift slope (5.7 per radian)
- v) blade chord at midpoint of the element or element station
- vi) air density
- vii) rotor speed in rad/sec
- viii) gravitational constant
- ix) x-ordinate of element stations

- x) flexured rigidity EI at element stations
- xi) vertical load at element stations

In the present case, the mass and damping matrices are diagonal matrices, hence they can be directly read into the program. The damping terms at each element station can also be calculated from the formula $\alpha \rho \frac{\Omega r}{2}$ (see equation 4.1.1). Depending upon the initial conditions at the hubjoint solve for M_1, M_2, \dots, M_{m-1} and $\theta_1, \theta_2, \dots, \theta_m$ from equations 4.1.6 and 4.1.8 by calling a matrix subroutine which computes the inverse and rank of a matrix and solves a set of simultaneous equations according to Gauss-Jordan reduction principle. Generate the matrix of influence coefficients, W_{1j} , from the recurrence relation 4.1.9. The stiffness matrix $[k_{1j}]$ is obtained by inverting the matrix $[W_{1j}]$.

With $[m]$, $[c]$, and $[k]$ matrices being generated in the first operation, call for matrix subroutines to compute

$$[m]^{-1}[c] \text{ and } [m]^{-1}[k]$$

and finally compute the eigenvalue matrix (see equation 3.6.8)

$$[G] = \left[\begin{array}{c|c} -[m]^{-1}[c] & -[m]^{-1}[k] \\ \hline [I] & [O] \end{array} \right]$$

The 2m eigenvalues and 2m eigenvectors are calculated in the following order:

- 1) Generating the characteristic polynomial. The subroutine is based on the Leverrier-Faddev method (20-355) according to which the coefficients p_1, p_2, \dots, p_n in the characteristic polynomial

$$\lambda^n - p_1 \lambda^{n-1} - p_2 \lambda^{n-2} - \dots - p_n = 0$$

are given by

$$p_n = (1/n)(\text{trace } [G_n])$$

where $[G_1] = [G]$

$$[G_n] = [G] \left[[G_{n-1}] - p_{n-1} [I] \right]$$

- 11) Calculation of roots of the characteristic polynomial:
This is effected by a subroutine of reference 20 which finds real and imaginary parts of complex roots and gives the reduced polynomial which in turn is examined for real roots if any.
- 11i) Solution of simultaneous linear equations for eigenvectors:
The complex modal columns or eigenvectors are obtained by a simultaneous equation subroutine (19, 22).
Presuming that the physical cross spectra $[S^f(\omega)]$

of the exciting system are known, the RMS deflection and stress values are computed in the following sequence:

- 1) Obtain the local force cross spectra from equation 4.4.19 and then transform it to the modal force cross spectra according to the relation 4.4.15.
- 2) From equation 4.4.16 compute the modal deflection cross spectra which when substituted in equation 4.4.17 gives the local deflection cross spectra.
- 3) Obtain the physical deflection cross spectra from equation 4.4.18.
- 4) Using any quadrature subroutine calculate the physical deflection and stress space cross correlation

$$[R^y(0)] = \int_{-\infty}^{\infty} [S^y(\omega)] d\omega$$

$$[R^{\sigma}(0)] = [S] [R^y(0)] [S]^T$$

the diagonal terms of which give the corresponding RMS values at element stations (refer to equations 4.4.20).